

**Argonne National Laboratory**

**REACTOR DEVELOPMENT PROGRAM**

**PROGRESS REPORT**

**December 1961**

### LEGAL NOTICE

*This report was prepared as an account of Government sponsored work. Neither the United States, nor the Commission, nor any person acting on behalf of the Commission:*

- A. Makes any warranty or representation, expressed or implied, with respect to the accuracy, completeness, or usefulness of the information contained in this report, or that the use of any information, apparatus, method, or process disclosed in this report may not infringe privately owned rights; or*
- B. Assumes any liabilities with respect to the use of, or for damages resulting from the use of any information, apparatus, method, or process disclosed in this report.*

*As used in the above, "person acting on behalf of the Commission" includes any employee or contractor of the Commission, or employee of such contractor, to the extent that such employee or contractor of the Commission, or employee of such contractor prepares, disseminates, or provides access to, any information pursuant to his employment or contract with the Commission, or his employment with such contractor.*

ARGONNE NATIONAL LABORATORY  
9700 South Cass Avenue  
Argonne, Illinois

REACTOR DEVELOPMENT PROGRAM  
PROGRESS REPORT

December 1961

Albert V. Crewe, Laboratory Director

<u>Division</u>	<u>Director</u>
Chemical Engineering	S . Lawroski
Idaho	M. Novick
Metallurgy	F . G. Foote
Reactor Engineering	B . I . Spinrad
Remote Control	R . C. Goertz

- - - - -

Report coordinated by R. M. Adams

Issued January 15, 1962





## FOREWORD

The Reactor Development Program Progress Report, issued monthly, is intended to be a means of reporting those items of significant technical progress which have occurred in both the specific reactor projects and the general engineering research and development programs. The report is organized in a way which, it is hoped, gives the clearest, most logical over-all view of progress. The budget classification is followed only in broad outline, and no attempt is made to report separately on each sub-activity number. Further, since the intent is to report only items of significant progress, not all activities are reported each month. In order to issue this report as soon as possible after the end of the month editorial work must necessarily be limited. Also, since this is an informal progress report, the results and data presented should be understood to be preliminary and subject to change unless otherwise stated.

The issuance of these reports is not intended to constitute publication in any sense of the word. Final results either will be submitted for publication in regular professional journals or will be published in the form of ANL topical reports.

The last six reports issued  
in this series are:

June 1961	ANL-6387
July 1961	ANL-6399
August 1961	ANL-6409
September 1961	ANL-6433
October 1961	ANL-6454
November 1961	ANL-6473



## TABLE OF CONTENTS

	<u>Page</u>
I. Water Cooled Reactors (040101)	7
A. General Research and Development	7
1. Irradiation Studies	7
B. EBWR	7
1. 100 Mw Modifications	7
2. Experimental Equipment	8
C. BORAX-V	8
1. Installation of Reactor and Components	8
2. Procurement and Fabrication	11
3. Design	13
4. Development and Testing	14
II. Sodium Cooled Reactors (040103)	17
A. General Research and Development	17
1. ZPR-III-Experimental	17
2. ZPR-III-Analysis	21
3. ZPR-VI and ZPR-IX	21
B. EBR-I	22
1. Fabrication of Core IV Fuel Elements	22
C. EBR-II	22
1. Reactor Plant	22
2. Sodium Boiler Plant	23
3. Power Plant	24
4. Engineering	25
5. Instrumentation and Control	26
6. Fuel Cycle Facility	27
7. Process Development	28

# TABLE OF CONTENTS

	<u>Page</u>
III. Reactor Safety (040117)	31
A. Thermal Reactor Safety Studies	31
1. Fuel-Coolant Chemical Reactions	31
2. Metal Oxidation and Ignition Kinetics	31
B. Fast Reactor Safety Studies	32
1. TREAT Program	32
2. Theoretical Studies	36
IV. Nuclear Technology and General Support (040400)	37
A. Applied Nuclear Physics	37
1. 3.0 Mev Van de Graaff	37
2. Argonne Thermal Source Reactor (ATSR)	40
3. $\bar{\nu}$ for $U^{235}$ and $Cf^{252}$	41
4. Fast Spectrum Measurements	41
5. Study of Resolving Loss Corrections for Scaler Data	42
6. High Conversion Critical Experiment	43
7. Theoretical Reactor Physics	44
8. Mathematical Numerical Methods Analysis	45
B. Reactor Fuels Development	46
1. Corrosion Studies	46
2. Nondestructive Testing	47
C. Reactor Materials Development	48
1. Radiation Damage in Steel	48
D. Heat Engineering and Fluid Flow	50
1. Boiling Liquid Metal Studies	50
2. Double Tube Burnout Study	50
3. Boiling from a Liquid-Liquid Interface	51
4. Two-Phase Nozzle Tests	51
5. Hydrodynamic Instability	51
6. Behavior of Fuel Plates in High Velocity Flow	52

## TABLE OF CONTENTS

	<u>Page</u>
E. Separations Processes	52
1. Fluidization and Fluorine Volatility Separations Processes	52
2. General Chemistry and Chemical Engineering	54
3. Chemical-Metallurgical Process Studies	55
F. Advanced Reactor Concepts	57
1. Fast Reactor Test Facility (FARET)	57
2. Direct Conversion Studies	59
V. Publications	61

# CONTENTS

## Page

1	Introduction
2	1. The first part of the book
3	2. The second part of the book
4	3. The third part of the book
5	4. The fourth part of the book
6	5. The fifth part of the book
7	6. The sixth part of the book
8	7. The seventh part of the book
9	8. The eighth part of the book
10	9. The ninth part of the book
11	10. The tenth part of the book
12	11. The eleventh part of the book
13	12. The twelfth part of the book
14	13. The thirteenth part of the book
15	14. The fourteenth part of the book
16	15. The fifteenth part of the book
17	16. The sixteenth part of the book
18	17. The seventeenth part of the book
19	18. The eighteenth part of the book
20	19. The nineteenth part of the book
21	20. The twentieth part of the book
22	21. The twenty-first part of the book
23	22. The twenty-second part of the book
24	23. The twenty-third part of the book
25	24. The twenty-fourth part of the book
26	25. The twenty-fifth part of the book
27	26. The twenty-sixth part of the book
28	27. The twenty-seventh part of the book
29	28. The twenty-eighth part of the book
30	29. The twenty-ninth part of the book
31	30. The thirtieth part of the book
32	31. The thirty-first part of the book
33	32. The thirty-second part of the book
34	33. The thirty-third part of the book
35	34. The thirty-fourth part of the book
36	35. The thirty-fifth part of the book
37	36. The thirty-sixth part of the book
38	37. The thirty-seventh part of the book
39	38. The thirty-eighth part of the book
40	39. The thirty-ninth part of the book
41	40. The fortieth part of the book
42	41. The forty-first part of the book
43	42. The forty-second part of the book
44	43. The forty-third part of the book
45	44. The forty-fourth part of the book
46	45. The forty-fifth part of the book
47	46. The forty-sixth part of the book
48	47. The forty-seventh part of the book
49	48. The forty-eighth part of the book
50	49. The forty-ninth part of the book
51	50. The fiftieth part of the book
52	51. The fifty-first part of the book
53	52. The fifty-second part of the book
54	53. The fifty-third part of the book
55	54. The fifty-fourth part of the book
56	55. The fifty-fifth part of the book
57	56. The fifty-sixth part of the book
58	57. The fifty-seventh part of the book
59	58. The fifty-eighth part of the book
60	59. The fifty-ninth part of the book
61	60. The sixtieth part of the book
62	61. The sixty-first part of the book
63	62. The sixty-second part of the book
64	63. The sixty-third part of the book
65	64. The sixty-fourth part of the book
66	65. The sixty-fifth part of the book
67	66. The sixty-sixth part of the book
68	67. The sixty-seventh part of the book
69	68. The sixty-eighth part of the book
70	69. The sixty-ninth part of the book
71	70. The seventieth part of the book
72	71. The seventy-first part of the book
73	72. The seventy-second part of the book
74	73. The seventy-third part of the book
75	74. The seventy-fourth part of the book
76	75. The seventy-fifth part of the book
77	76. The seventy-sixth part of the book
78	77. The seventy-seventh part of the book
79	78. The seventy-eighth part of the book
80	79. The seventy-ninth part of the book
81	80. The eightieth part of the book
82	81. The eighty-first part of the book
83	82. The eighty-second part of the book
84	83. The eighty-third part of the book
85	84. The eighty-fourth part of the book
86	85. The eighty-fifth part of the book
87	86. The eighty-sixth part of the book
88	87. The eighty-seventh part of the book
89	88. The eighty-eighth part of the book
90	89. The eighty-ninth part of the book
91	90. The ninetieth part of the book
92	91. The ninety-first part of the book
93	92. The ninety-second part of the book
94	93. The ninety-third part of the book
95	94. The ninety-fourth part of the book
96	95. The ninety-fifth part of the book
97	96. The ninety-sixth part of the book
98	97. The ninety-seventh part of the book
99	98. The ninety-eighth part of the book
100	99. The ninety-ninth part of the book
101	100. The hundredth part of the book



## I. WATER COOLED REACTORS (040101)

### A. General Research and Development

#### 1. Irradiation Studies

a. Postirradiation Annealing of Al-17 w/o U Alloy and Al-39 w/o (U<sub>3</sub>O<sub>8</sub>) Dispersion - There are many criteria for judging potential reactor fuel materials. One characteristic which is common to all is dimensional stability under irradiation. Since metallic fuels exhibit a temperature at which large volume increases occur in a relatively short time, i.e., the swelling temperature, operation at or above this temperature is not feasible. The useful operating temperature can be extended by suitable cladding or jacketing of the fuel core. However, there are practical limitations on the amount of restraint that can be incorporated into a fuel element design. Thus a knowledge of the swelling temperature limitations of the fuel is essential.

In order to obtain this type of information on some aluminum-base fuels a series of annealing studies on irradiated Al-17.5 w/o U alloy and Al-39 w/o U<sub>3</sub>O<sub>8</sub> dispersion coupons was initiated. The dispersion specimens had between 0.0005 in. and 0.003 in. of aluminum cladding on two faces of the coupons and none on the edges. The alloy specimens were clad with approximately  $\frac{1}{32}$  in. of aluminum on their faces and  $\frac{1}{4}$  in. on two edges, the remaining two edges having no restraint. The annealing studies were conducted in a salt bath.

The data indicate that for burnups equal to or less than  $1.6 \times 10^{20}$  fiss/cc, the Al-17.5 w/o U alloy specimens clad with  $\frac{1}{32}$  in. of aluminum have excellent resistance to swelling at temperatures up to 550°C. However, for specimens with burnups of  $5.5 \times 10^{20}$  fiss/cc swelling does occur at 550°C.

For the Al-39 w/o (U<sub>3</sub>O<sub>8</sub>) dispersion specimens the data also indicate excellent resistance to swelling for burnups equal to or less than  $1.35 \times 10^{20}$  fiss/cc and temperatures up to 500°C.

### B. EBWR

#### 1. 100 Mw Modifications

a. Reboilers - Insulation of the primary reboilers, piping, and auxiliary equipment has been completed. It is expected that the reboiler plant will be ready to operate the first week of January 1962.

b. Instrumentation and Control - A checkout of the instrumentation and control systems of the reboiler building is in progress. Pneumatic control systems are being checked for proper functional operation and adjusted for mid-range control points. Annunciator limit switches are being checked for proper settings.

c. Change of Control Rods - The fueled follower control rods were replaced with rods having Zircaloy-2 followers. This replacement was made in order to improve hydrodynamic conditions by eliminating instability that may have arisen from insufficient cooling of the fueled followers.

## 2. Experimental Equipment

a. Transfer Functions - A start-stop logic circuit has been designed to operate the analog computers to be used in EBWR dynamics studies. A manual control will be able to start both the analog and the digital unit at the beginning of a cycle and stop after a desired number of cycles. The analog computer will be switched to a "compute" mode at the start of operation, and to a "hold" mode to allow recording when it stops. A clock operated by the computer is used to indicate total computing time. The test circuit has been built and tested.

b. Neutron Flux Distribution in EBWR - Design of the modification of the East Instrument Nozzle has been completed (see Progress Report, November, 1961, ANL-6473) and fabrication of components has been initiated.

A machine for fabricating lengths of bead chain with special segments containing flux measuring foils has been built. Chains containing cobalt and gold monitoring materials at fixed intervals are being prepared for use in EBWR.

It has been found that tubing loops through the reactor can be rethreaded with bead chain should a break in the chain occur. A device has been constructed which uses air pressure to accomplish the rethreading operation.

c. Demister Test - After one week operation in a steam loop, a stainless steel wire mesh demister sample showed considerable fracturing of the wire mesh.

## C. BORAX-V

### 1. Installation of Reactor and Components

Following completion of the first phase of preoperational testing on the reactor systems at operating temperature (489°F) and pressure (600 psig), the reactor vessel head, boiling core structure and other reactor vessel internals (steam collector, feedwater sparger, control-rod-drive nozzle shield plugs, and superheated steam nozzle caps) were removed.

The 24-junction downcomer differential temperature thermopile, 3 reactor water and 2 steam temperature thermocouples, 3 capsules containing reactor-vessel-steel samples with integral monitoring thermocouples, and a thimble for reactor vessel flux monitors were installed on the east wall of the reactor vessel. Placement of these items completed the installation of permanent in-vessel instruments. Figure 1 shows the reactor vessel with these items installed. Recorders associated with the above temperature and pressure detectors are installed, and the wiring and external instrument piping is nearing completion. Cooling water lines for the downcomer DP probes were completed and hydrotested.

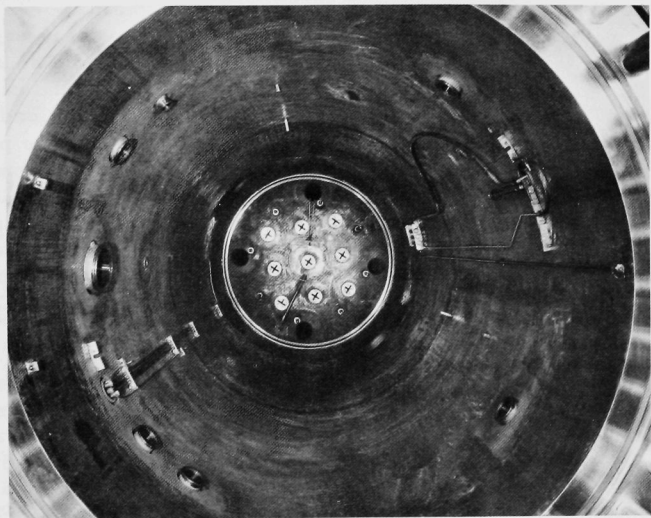


Figure 1

Interior of Reactor Vessel with Permanent In-Vessel Instruments Installed.

The reactor vessel interior, forced-convection system inlet and outlet nozzles and piping, control rod drive nozzles and plugs, and the forced-convection pump casing were swabbed and flushed to remove the residual rust film and loose particles resulting from operation at temperature.

All nine control rod drive mechanisms, seals and dashpot housings were removed, disassembled and cleaned. The valve disc and seat in the dashpot housing was reground, and leak-tested satisfactorily. The seal water leakoff tubing has been revised to accommodate thermocouples for monitoring the temperature of each seal.

The boiling core structure and the lower feedwater sparger and forced-convection baffle were reinstalled in the reactor vessel. The control rods of the original design, to be used for the initial cold critical operation with the boiling core, were received, straightened (see below) fitted to the dashpot latches, and installed in the core structure. Figure 2 shows a control rod being installed. The control rod drive dashpots,

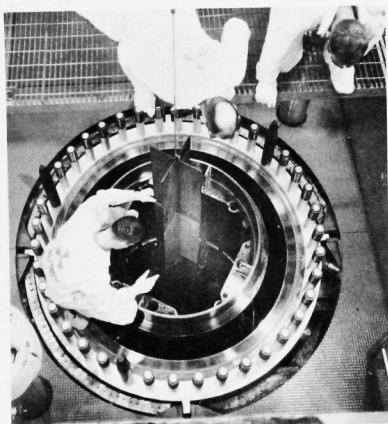


Figure 2

Boiling Core Structure In Place. Control Rod Being Installed.

seals, mechanisms, selsyns, drive motor assembly and associated piping, tubing and wiring were reinstalled, connected to control rods, adjusted and checked out.

The reactor vessel was filled with water, and the Sb-Be source was installed in the reactor and used to check out the two in-core loading counter circuits and the five permanent nuclear instrument channels. With the receipt of an additional 2,025 boiling fuel rods (a total of 2,425 rods are now on hand at the reactor site) the reactor is technically ready to begin loading for initial cold criticals on short notice.

While awaiting hazards approval, modifications and preoperational testing in preparation for power operation are continuing. The forced-circulation piping has been connected in preparation for the measurement of flow distribution across the core under forced circulation conditions. At the suggestion of the AEC, Division of Licensing and Regulation, the time required to open the forced-convection system discharge valve has been changed from one to two minutes by installing a half-speed motor on the valve operator.

Installation of an additional 168 kw to the electrical preheating system in the form of strip heaters on the auxiliary water piping has started. Conduit and terminal boxes have been installed. This makes a total of 312 kw of electrical preheating and should reduce the time required to achieve operating temperature and pressure to less than 15 hours under natural circulation conditions. Modification of the boron tank piping and heating system to improve temperature distribution is also in progress. Leaking valve packings and valve seats discovered in the at-temperature tests have been repaired or replaced.

To help keep water off the control rod drive mechanisms, low coamings have been installed around each pipe or nozzle hole in the floor of the reactor pit, except one which was converted to a drain. Also, a protective "rain cap" cover with drain has been installed over each rod-drive position-indicating selsyn. For proper functioning of the reactor pit ventilation system, debris has been removed from the piping sleeves in the floor of the reactor pit.

An exhaust fume hood was installed on the regenerating tank of the makeup water demineralizer and a resin catch screen on the inlet to the makeup water storage tank.

The TV system for remotely observing the reactor-water-level sight glass and pressure gauge has been installed and is operative. The amplifier-scaler circuit for two in-core loading counters has been installed.

## 2. Procurement and Fabrication

a. Superheater Fuel - Of the 380 central superheater enriched plates received at Argonne, Illinois, 190 Type HCE (half-enriched central) have been inspected with only two rejected and 76 Type FCE (fully-enriched central) have thus far been inspected with no rejections. Two hundred sixteen Type HPE (half-enriched peripheral) plates have also been received and 80 Type FCE plates have been fabricated and are being inspected at the supplier's plant.

Dilatometry tests have been completed on eight samples cut from assembly development plates. Data from the resultant curves are being analyzed to determine the thermal expansion coefficient and to compare the expansion of fuel plates containing dispersion type core material with Type 304 stainless steel and the Type 304-L cladding material.

A successful braze of three, 4-plate superheater fuel elements using plates containing depleted  $\text{UO}_2$  was made in one fixture. One of these fuel elements is being autoclaved to check for warpage. Another was sectioned to inspect brazed joints. The brazes and spot welds between spacer wires and fuel plates were found to be excellent. The brazed joints between fuel plate edges and side plate grooves were found to have an occasional small ( $\frac{1}{8}$  in.) unbrazed gap. These gaps were too few to affect the strength of the element.

The newly installed Glo-Bar furnace was used for this brazing. A second furnace has arrived and installation has begun. Preparations are being made to try a five-element braze with a more rapid cool-down cycle. With the exception of the Inconel-X hold-down springs, all non-fueled components of the superheater fuel assemblies have been completed or received from vendors and are ready for assembly.

A third two-week corrosion test in 300°C water on 12 assembly development plates has been completed. Of main concern in these tests was the presence of rust spots which encircled pitted areas. The extent of reaction around these areas after the third test was no more severe than after the first test. After each of the first two tests a given number of corroded areas were scraped clean. Subsequent tests showed no additional attack at these areas thus indicating that the reaction is superficial.

Testing of stainless steels of interest (Types 304, 316, 347 and 406) has continued in superheated steam at 650°C and 600 psi, generated from high purity water with an initial oxygen content of about 27 ppm (effluent contains about 20 ppm). Maximum exposure to date is about 25 days. There are indications that the corrosion rate is decreasing with exposure time.

b. Reactor Components - Nine boiling core control rods of the original design were completely assembled, inspected and shipped to Idaho along with two spare poison sections. Procurement of materials for superheating core control rods of revised design was completed and fabrication of the end closure pieces has started.

Nine 17-4 PH stainless steel control rod extension shafts have been given final heat treatment, centerless ground, and are now ready for chrome plating and finish honing.

Another hold-down Belleville spring for the natural convection core structure has been fabricated from 17-4 PH stainless steel and has been calibrated for loads up to 30,000 lb. To adjust the Belleville spring deflection, 0.040 in. was machined from the lower Stellite overlaid bearing ring.

c. Experimental Components - Mechanical assembly of the duplex flux wire counter is essentially completed and fabrication of electronic components is well advanced. The liner and tank for the BORAX V exponential experiment are being modified to fit in TREAT.

To date, seven high-temperature Ta-sheathed W-W/26% Re thermocouples have been successfully brazed into boiling thermocouple rods. The  $\text{UO}_2$  in these rods was degassed by heating in a vacuum and the rods purged and filled with a pure He atmosphere during the welding and brazing operation. It is hoped that the Ta thermocouple sheath will survive better under these conditions at high temperatures. With the exception of the latches for the exit flow meters, all other components for the instrumented boiling fuel assemblies are completed. Fabrication of special pitot tubes for the forced-circulation core flow distribution tests was completed. Fabrication of the fission product monitor for superheated steam is nearly complete. Fabrication of the remotely controlled reactor-vessel-steam-dome sampling probe has started.



### 3. Design

When the nine control rods of the original design were received at the reactor site, they were found to be slightly bent (as a result of handling and free storage) in the 3 in. aluminum cruciform extension section. The calculated maximum handling or horizontal storage stress on this section is only about 2,000 psi which, unexpectedly, is apparently too high for the soft X-8001 aluminum. This alloy has a reported yield strength of 18,700 psi at room temperature. The design of the new superheating core control rods is being revised to eliminate this 3-in. aluminum section by extending the 3 in. stainless steel cruciform section up to the 14-in. aluminum follower with the mechanical joint on the follower.

Detailed design continued on the oscillator rod drive, the fuel rod gamma scanning machine and the in-core flux monitoring thimbles. Detailed design was started on the remotely controlled reactor-vessel-steam-dome sampling probe which will also be used during initial cold and hot zero power operation to insert and withdraw the Sb source from the Be cylinder in the core.

As a result of the apparent high corrosion and scaling rate recently reported on Type 304 L stainless steel in 1,200°F superheated steam containing 30 cc/liter of O<sub>2</sub>, a study has been initiated to seek a means of greatly reducing the oxygen content of the saturated steam in the reactor steam dome before it enters the superheater fuel assemblies. The feasibility of a full flow, in-vessel, catalytic recombiner is being first investigated.

The proposal to run a subcritical exponential experiment on BORAX V fuel for study and calibration of steam void measuring techniques has been redrafted to meet the special requirements of the TREAT facility. It was shown that an adequate and safe assembly can be achieved with 349 fuel pins in a cylindrical array surrounded with cadmium.

Previous calculations made for various operating conditions are being critically examined in order to establish the range of probable epithermal-to-thermal flux ratios.

A criticality analysis of the superheater fuel storage rack is being made. The present plan calls for the construction of 45 cadmium-lined boxes to be installed in the old BORAX reactor vessel.

A series of PDQ cell problems were run in order to examine the effect of various assumptions used in the control rod worth calculations. These are based on a unit cell consisting of four homogenized boiling fuel assemblies surrounded with either steel and water, Boral, or an aluminum follower and water. The reduction of rod worth by replacing a corner fuel rod with a boron-stainless steel rod is represented by homogenizing the composition in an equivalent, but small square area. The corresponding eigenvalues are given in Table I.

Table I. Eigenvalues of 3-Group PDQ Control-Cell Problems

Cell Conditions	$k_{eff}$ cell	Equivalent $k_{eff}$ for boiling core*
1. Aluminum follower and water surrounding cell, cold, no poison rods	1.2803	1.229
2. Control rod material and water surrounding cell, cold, no poison rods. Extrapolation length, 2.15 cm	0.9365	
3. Control rod material and water surrounding cell, cold, B <sup>10</sup> smeared in fuel region (Same composition as used previously to give a $k_{eff}$ of 1.03 hot and 15% average voids.) Ext. length into control rod, d = 2.15 cm	0.9468	0.874
4. Control rod material and water surrounding cell, boron-S.S. rod in corner, cold	0.9332	
5. Follower and water surrounding cell, boron-S.S. rod in corner, cold	1.264	
6. Logarithmic boundary on control rod based on ratio of leakage flux-to-flux from SNG detailed slab problem and applied in epithermal and thermal groups. [Compare with (2).]	0.9209	
7. Boiler cell, hot 15% voids, control rod and surrounding, d = 2.15 cm	0.8808	

\*Corresponding values for reactor problems

#### 4. Development and Testing

a. Control Rods - Development work continued on the dimpled cladding concept of the revised control rod design. The first attempt at furnace annealing a sample angle of cladding caused warpage in the arm which did not have an edge flange. Another anneal is being tried with a temporary edge flange on this arm and a better annealing fixture. A new spot-welding machine has been installed for making the cladding spot welds.

b. Control Rod Drive Seals - As a result of high leakage through the seals during the at-temperature preoperational tests on control rod drives, additional tests were run on each seal, using a pressure of 600 psig and cold water. The extension shafts were tested in two positions, because the shaft is stepped. The measured leak rates varied from about 9 to 70 gallons per hour. Accurate measurements of the inside diameter of the seal rings

showed that three seal rings, out of a total of 45, exceeded the design diameter. Two of the in-tolerance rings seemed corroded or pitted. The defective seal rings will be replaced and the tests repeated with the new control rod extension shafts when available.

c. In-Core Instrumentation Development - The high temperature test contract with Thermatest Laboratories has been completed, and tests indicate that the Ta-sheathed, BeO-insulated, W-W/26% Re thermocouples are useable for temperatures up to 4,000°F. On 2 of the 8 samples tested the sheath at the welded junction separated from the balance of the assembly without destroying the junction, but with unpredictable results on the emf vs. temperature curve. This effect, and the 4,000°F temperature limitation owing to a reaction between BeO and Ta, are the only apparent deficiencies in the thermocouple design. Thus it should be possible to use these thermocouples for obtaining data on the boiler for long-term operating periods at power levels up to 20 Mw, and for shorter periods of time at power levels to 40 Mw with a suitable choice of fuel rod location.

The brazing procedure for the thermocouple lead pressure seals at the pressurized terminal box is the last fabrication problem yet to be solved. Induction heating has not been satisfactory to date, and a resistance furnace is now being investigated.

Calibration of one steam flow riser venturi for an instrumented superheater fuel assembly has now been completed by Alden Hydraulic Laboratory (Worcester Polytechnic Institute). Data will be used to correct the performance of the venturi tubes installed in other instrumented super-heat fuel assemblies.

d. Plant Tests - Preoperational tests were continued. On the second attempt, the reactor vessel and associated systems were brought to operating temperature and pressure using the electric preheat system. The previously reported difficulties with the auxiliary pump packing were corrected by maintaining the seal water pressure 30-50 psi above reactor pressure. Test operation of the control rod drives showed the need for control of seal water pressure to maintain satisfactory performance of the seals.

Excessive steam hammer was found in the feedwater piping when feedwater flow was stopped for any appreciable length of time while the reactor was at pressure. This is to be corrected by locating a spring loaded piston check valve in the horizontal run of the feedwater line from the reactor vessel immediately after the line goes through the shield wall. The boron addition system also had excessive steam hammer because of the layer of cold water in the bottom of the tank. The electric heating equipment for this system is being modified to keep the tank solution at the same temperature as the reactor by the addition of heaters to the bottom of the tank, by the addition of heating tape on the water level gauge glasses and by the addition of more control circuits.

Due to steam hammer, the batch feed system required an excessive amount of time for addition of water. A steam sparger is to be installed to heat the tank water with reactor steam before adding the water to the reactor vessel.

Tests of the reactor vessel relief valves were satisfactorily completed. Testing of the superheater drain system produced excessive pipe movement, indicating a need for additional guide anchors.

Tests were performed on the forced-convection pump seal flow control system. Performance of the controller was found to be satisfactory if the supply pressure is kept below 200 psig when there is atmospheric pressure in the pump. Under these conditions, the seal water input can be maintained constant at from 2 to 4 gpm per seal. The new seal water-pressure-control system will be designed to keep the supply pressure within the range of the controller. The quench valve can maintain pressure at 35 psig or less for supply pressures from 35 to the maximum available pressure with resulting return flow of 1 to 2 gpm.

## II. SODIUM COOLED REACTORS (040103)

### A. General Research and Development

#### 1. ZPR-III-Experimental

Work continued this month on Assembly 35, the mockup of APDA Fermi core B. Experiments included axial traverses, worths of safety and oscillator rods, and the investigation of various radial reflectors.

Central fission ratios were measured for several isotopes as part of the effort to evaluate the effects of counter wall-thickness on the measured values. Data are still being analyzed.

a. Reactivity Coefficient Measurements - Previous measurements had indicated the worth of nickel to be greater than stainless steel at all locations except the center. The central reactivity coefficients of Ni, Fe, and stainless steel were therefore measured to check the low value previously measured for nickel. The results, given in Table II, verify the previous measurements.

Table II. Central Reactivity Coefficients

<u>Material</u>	<u>Mass (kg)</u>	<u>Worth (lh)</u>	<u>Reactivity Coefficient</u> <u>Inhours per kg.</u>	<u>Previous Value</u> <u>Inhours per kg.</u>
Armco Fe	1.028	1.0	1.0	1.0
Ni	1.1504	0.5	0.43	0.41
SS	1.0186	1.0	1.0	0.9

b. Safety Rod Measurements - A Fermi B safety rod was simulated and its worth measured as a function of position throughout the core. The Fermi B safety rod channel is 2.7 in. square. This was simulated by loading  $1\frac{1}{2}$  drawers of the 2-in.-square ZPR-III matrix with sodium-filled stainless steel cans. The boron carbide was then loaded into these drawers in steps. The measurements were made by the difference in critical position of the ZPR-III control rod as the mockup rod was inserted toward the core midplane, and by subcritical extrapolation in the second half of the core. The results are given in Table III.

Table III. Worth of a Safety Rod

Boron Content: 28.63 gm of B<sup>10</sup> per 5.08 cm.  
19.65 gm of B<sup>11</sup> per 5.08 cm.

#### Worth Measurements:

<u>Substitution Location (in.)</u>	<u>Reactivity Worth (lh)</u>	
32 to 18 (axial blanket)	- 14.5	
18 to 14	- 30.5	
14 to 9	- 73.7	
9 to 7	- 37.9	Critical Measurements
7 to 4	- 66.2	
4 to 2	- 47.2	
2 to 0	- 48.4	
Total to core midplane	-318.4	
0 to - 7	-168.9	Subcritical Measurements
0 to -18	-312.2	

c. Oscillator Rod - An oscillator rod 35 in. long, containing natural boron carbide was constructed to fit the 2-in.-square ZPR-III matrix. The average worth of the oscillator and its wave shape were measured in each of two core positions to allow extrapolation to the 2.7-in.-square subassembly size of Fermi B. The worth of the oscillator was measured relative to sodium. The results are given in Table IV.

Table IV. Oscillator Rod Measurements

Composition

SS	- 332.267 gm
Al	- 80.076
B <sub>4</sub> C	- 615.731 (76.98 w/o B, 19.2 a/o B <sup>10</sup> )

Worth

Location	1-P-19	1-P-20
Average Radius (cm)	16.5	22.0
Average Worth (Ih)	-131.1	-124.4

<u>Wave Shape</u>			
<u>Angle (°)</u>	<u>Worth (Ih)</u>	<u>Angle (°)</u>	<u>Worth (Ih)</u>
-7.5	-0.53	-10	-0.76
32.5	1.42	- 1	-0.05
52.5	3.22	9	0.72
82.5	4.02	29	2.26
112.5	3.58	49	3.52
142.5	2.36	69	4.58
172.5	0.45	79.5	4.71
202.5	-1.39	89	4.73
232.5	-2.93	109	4.51
262.5	-3.54	129	3.65
272.5	-3.66	149	2.42
292.5	-3.26	169	0.86
323.0	-2.19	179	0.09
2.5	0.16	189	-0.58
92.5	4.00	209	-1.99
		229	-2.95
		249	-3.68
		259	-3.87
		269	-3.85
		280	-3.85
		289	-3.70
		309	-3.05
		329	-2.14
		349	-0.74
		99	4.72



d. Reflector Experiments - Three different reflectors were constructed, and materials substitutions were performed to obtain sufficient data to allow APDA to optimize the radial reflector. A one-row Ni reflector was constructed in a  $\frac{1}{4}$  segment of half the core. The substitution experiments were performed by replacing one  $\frac{1}{4}$ -in. Ni column with the desired material. A  $\text{Ni}_2\text{O}$  reflector and an iron oxide reflector were then built in the same segment. Substitutions were performed in the iron oxide reflector by replacing one  $\frac{1}{8}$ -in.  $\text{Fe}_2\text{O}_3$  column and one  $\frac{1}{8}$ -in. stainless steel column with the desired material. In part A of Table V the actual compositions used for the reflectors are given. The values in part B of Table V are relative to void.

Table V. Reflector Experiments

A. Reflector Compositions (gm/cm<sup>3</sup>)

<u>Constituent</u>	<u>Nickel</u>	<u>Iron Oxide</u>	<u>Nickel Oxide</u>
Ni	5.44		2.72
Na	0.159	0.159	0.159
SS	0.954	1.35	2.03
Fe	-	1.74	
O	-	0.692	0.428

B. Substitution Experiments Worths (Ih/kg)

Ni	1.6	2.0	-
SS	1.5	1.6	-
Na	7.8	5.7	-
Fe	1.4	1.4	-
$\text{Fe}_2\text{O}_3$	3.0	2.9	-
O(cal.)	7.0	6.6	-

C. Calculated Worth of a Complete Reflector 2.8 in.-thick

Ni/fine radial Blanket	+1,302 Ih
NiO/Ni (from nickel reflector measurements)	+40
(from iron oxide reflector measurements)	+24
(from nickel oxide reflector measurements)	+87
$\text{Fe}_2\text{O}_3/\text{Ni}$	+52

e. Axial Traverses - Reaction rate traverses were taken along the central core axis for  $\text{U}^{235}$ ,  $\text{U}^{238}$ ,  $\text{Pu}^{239}$ , and  $\text{B}^{10}\text{F}_3$ . The traverse position indicates the center of the active volume which is 2 in. long for these counters. The results are summarized in Table VI. A  $\frac{1}{2}$ -in.-long  $\text{U}^{235}$  and 2-in.-long  $\text{U}^{238}$  sample were also traversed through the same mechanism. The worths were determined by subtracting the worth of the mechanism

from the worths of the mechanism-plus-sample as determined from the difference in control rod positions. The data are given in Table VII.

Table VI. Reaction Rate Traverses Through Axial Centerline

Edge of Blanket at 13.0 in.  
Edge of Core at 27.0 in.  
Core Midplane at 45.0 in.

Counts per 1,000 counts on standard counter

<u>Traverse Position, in.</u>	<u>U<sup>235</sup></u>	<u>U<sup>238</sup></u>	<u>Pu<sup>239</sup></u>	<u>B<sup>10</sup>F<sub>3</sub></u>
13	250.7	0.905	87.0	2267
21	1586.2	13.8	466.5	8105
25	2963.3	53.5	855.9	14245
27	3814.7	110.2	1111.2	17997
28	4248.6	150.0	1313.1	19531
29	4671.7	191.3	1418.2	22255
31	5409.0	239.9	1629.7	24753
33	6207.5	274.4	1930.5	28601
37	7318.1	349.9	2222.2	33228
39	7694.7	367.1	2355.6	34236
41	8131.9	374.8	2436.1	35931
42	8109.6	385.4	2458.8	36988
43	8245.9	387.1	2567.6	37290
44	8304.5	396.7	2528.9	36530
45	8292.8	382.2	2566.4	37842
46	8390.0	392.2	2593.9	36996
47	8130.8	389.0	2539.7	36789
48	8295.1	-	2471.2	-
49	8082.1	377.8	2515.6	36925
51	7838.9	-	2372.3	-
53	7308.4	351.0	2327.5	-

Table VII. U<sup>235</sup> and U<sup>238</sup> Reactivity Worth Traverses

Edge of Blanket at 13.0 in.  
Edge of Core at 27.0 in.  
Core Midplane at 45.0 in.

<u>Traverse Position, in.</u>	<u>U<sup>235</sup> Worth (1h)</u>	<u>U<sup>238</sup> Worth (1h)</u>
0	0	0
17	0.01	0.02
21	0.24	0.06
25	0.43	0.11
27	0.57	0.08
28.5	0.85	0.08
30	0.91	0.14
33	-	-0.08
36	1.52	-0.11
39	-	-0.26
42	2.04	-0.26
45	2.11	-0.21
48	1.99	-0.26
54	1.52	-0.13
60	0.85	+0.08
61.5	0.77	-
63.0	0.57	-

## 2. ZPR-III-Analysis

The effective  $k$  and the surface neutron flux of the subcritical plutonium-fueled ZPR-III assembly No. 37 (see ANL-6399, Monthly Progress Report for July 1961, for description) has been calculated using two groups and the TDC neutron transport code in R-Z geometry. The effective  $k$  is calculated to be about 0.5. The surface flux density at the center of the exposed core face is calculated to be about 800 neutrons/(cm<sup>2</sup>)(sec). About 28% of this flux represents neutrons of energy above the threshold for U<sup>238</sup> fission.

## 3. ZPR-VI and ZPR-IX

a. Building - The concrete walls of the reactor cells have been found to be quite porous. With the cells pressurized to 0.68 bars (10 psig) there is a leakage rate of about 23% of the volume per 24 hours for Cell No. 4 and 10% of the volume per 24 hours for Cell No. 5. Since these leakage rates are excessive, it has been decided to coat the interior walls of the cell with a phenolic resin-base paint to make the cells more gas-tight. The installation of the wiring and assembly of the reactor are being postponed until after the completion of the painting since a great deal of dirt and dust will be produced in the cells during surface preparation.

b. Bed and Table Assembly - Components such as an air filter and a pressure switch for the emergency air motor drive system were mounted on the bed below the movable table surface for protection. Copper tubes were run to an air supply.

The entire bed and table assembly is now covered with polyethylene sheeting for protection from dirt and dust expected during preparations for the painting of the cells. The assembly is now in place but not wired. Final installation work is postponed until after the painting.

c. Matrix Assembly - Approximately 75% of the matrix tubes have been bundled and welded into 5 x 5 tube units. Excellent dimensional accuracies are being met. These completed units are now stored until final assembly on the reactor is started. Eighty percent of the drawers for the matrix assembly have been fabricated and are ready for use.

Experimental work on the aluminum tubes for ZPR-IX which do not meet specifications continues. Some of the tubes which were stress-relieved at 350°F for two hours and then drawn showed promise for successful sizing.

d. Control and Safety Rods - Difficulties encountered by the supplier during final assembly have been overcome and the first two drive units are expected early in January 1962. The units will then be wired and checked out by Laboratory personnel.

e. Control Console and Instrumentation - The second control console and its instrumentation was received from the supplier. The console has been moved into the control room in preparation for final wiring installation. The first console received, which is located in the Cell No. 4 control room, is being wired to the reactor cell terminal boards. Final wiring between the terminal boards and the reactor will be delayed until after the completion of the painting of the cells.

The individual testing instruments of the control console of Cell No. 4 are about 50% complete. Thus far only minor deviations from specifications have been found.

## B. EBR-I (41412-01)

### 1. Fabrication of Core IV Fuel Elements

A total of 555 Core IV fuel and blanket rods are being fabricated for use in EBR-I. This number includes 420 fuel rods, 120 blanket rods, 10 fuel thermocouple rods and 5 blanket thermocouple rods.

Assembly operations have been temporarily suspended pending additional procurements. An order has been placed with Superior Tube Company for 250 feet of Zircaloy-2 jacket tubing for the additional fuel rods required. Mid-January shipment has been promised.

As a backup effort to procurement of commercial tubing, sufficient base tubing was extruded at ANL to fabricate an estimated minimum of 125 jackets. A total of 76 jacket tubes are in process.

Finished machined and numbered rod tips for the bottom end closure of 100 jacket tubes have been completed.

Defect-free rib wire stock has been fabricated at ANL from Bureau of Mines zirconium. Sufficient  $\frac{1}{16}$  in. diameter rib wire stock has been drawn, straightened and cut to length for 103 jacket assemblies.

The required amount of 0.080 in. OD Zircaloy-2 instrument tubing has been fabricated and annealed prior to straightening, nondestructive testing and final pickling.

## C. EBR-II

### 1. Reactor Plant

All of the subassemblies have been unloaded from the reactor and transferred to the Lab and Service Building. The fuel has been stored in a special materials vault and the blanket material is stored in the basement.

Minor operational difficulties encountered during the dry critical experiments will be corrected in preparation for the forthcoming wet critical experiments.

Representative items of work in this area are installation of protective boots over the threaded shafts of the reactor vessel cover locking mechanisms, repairs of leaking oil seals on the reactor vessel cover lifting mechanism, installation of sight glasses for observation of the oil level in the shock absorbers on the control rod drives, and modifications of the safety rod storage holes in the storage basket.

Installation of the sodium purification cell periscope and shield has been completed. The nuclear instruments have been removed from the thimbles for the forthcoming elevated temperature test of the primary tank.

Various malfunctions have been observed in the operation of the numerical positioning system. The following were rectified:

- (a) Incorrect circuit action with respect to the small rotating plug overtravel signal.
- (b) The possibility of incorrectly positioning the rotating plugs to a point an integral number of thousands of counts from the correct position.
- (c) Incorrect positioning of the large rotating plug nine counts from the correct position.
- (d) Incorrect punching of output cards as a function of digital clock numbers.

The rotating plug primary position transducers are being calibrated against the secondary transducers. This will permit a more accurate adjustment of the associated error encoders.

A spare festoon cable for the large rotating plug has been received and inspected. The components and circuits required for motor operation of the gripper jaws on the refueling machine have been installed. Indicating lights associated with the cooling duct connections were also installed.

## 2. Sodium Boiler Plant

The two superheater units were delivered to the site. They have been raised into place and leak tested with a helium mass spectrometer. No leaks were found. Installation of these units is proceeding.

Evaporator B3-EB702 has been repaired and is being readied for shipment to the site.

Installation of piping for the unloading of sodium from the ten tank cars is well along. The tank cars are located on cribbing north of the Sodium Boiler Building as shown in Figure 3. All the tanks will be completely piped prior to unloading because it is not desirable to make any sodium piping connections during the unloading operation.

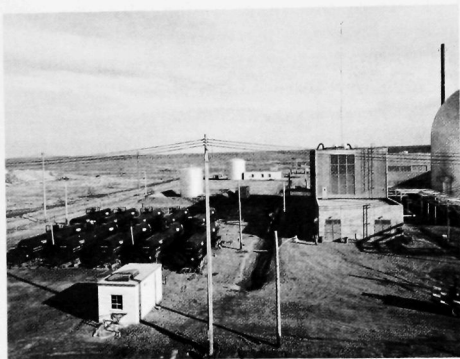


Figure 3  
Tank Cars of Sodium for EBR-II

The Dowtherm system for cooling the secondary cold trap was successfully test run. Thermocouple wells were welded to the shells of the eight evaporators, and considerable progress was made on other miscellaneous deficiency work. Modification, repair, and checkout of the secondary sodium system control panel was completed as far as possible at this time.

Chemical analysis of the special heliarc stainless steel weld rod showed the nickel content too high and therefore, out of specification requirements. To meet the ferrite content requirement for the deposited weld metal as well as the chemical requirements, it was decided to change the welding procedure from inert gas tungsten arc to a procedure that uses inert gas tungsten arc welding for the root pass and metallic arc for subsequent passes. Weld rod for this procedure was received and test pads for chemical analysis are being prepared.

### 3. Power Plant

The turbine supplier's field engineer arrived early in the month and supervised final preparation and alterations for running the turbine-generator with 175-lb steam supplied from the auxiliary heating boilers. The blowdown line was connected from the turbine stop valve through the north wall of the building and the steam lines up to the stop valve were blown down with steam. The control linkages in the turbine front standard were set and all pressure switches and interlocks on the machine were correctly adjusted.



Following this preliminary work, 175-lb steam was admitted to the turbine and the machine was brought up to speed. The high-speed stop was set and both the low-oil-pressure trip and the overspeed trip were tested.

Following this operation, inspection of the interior of the turbine revealed that the protective compound (rust preventive shipping compound) had been successfully removed. At this time, the initial pressure governor was placed in operable condition by the field representative. Except for final setting when 1250-lb steam is available, the turbine control system is now ready for service.

During the initial operation of the turbine, the bearing header oil strainers became plugged with lint and other foreign material and required operation of the auxiliary oil pump while the unit slowed down and cooled off. These oil filters were subsequently cleaned and operated satisfactorily during later operation. Preparations are in progress to remove the turbine oil, clean the storage tank, and filter the oil while refilling. It was also necessary to open, inspect and clean the water side of the turbine oil coolers.

#### 4. Engineering

a. Primary Tank - Measurements of the over-all spring constant of the primary tank (described in ANL-6473, Monthly Progress Report for November, 1961) have been completed and preliminary analysis of the results show a good agreement with the predicted value. Devices are now being installed to measure the vertical displacement of the primary tank cover relative to the top structure at elevated temperatures. Results from the elevated temperature measurements, together with the spring constant measurement, will allow very accurate determination of the effect of the sodium load on relative positions of the fuel handling equipment and reactor.

b. Analysis - The measured fission distributions in the outer portions of the outer blanket of the reactor appear to be higher than predicted. Furthermore, the neutron flux leaving the radial neutron shield has a higher intensity and a softer spectrum than predicted. It is concluded that the neutron spectrum in the outer blanket is softer than predicted. This observation is similar to that found in other fast reactors.

Shielding calculations of neutron fluxes in the primary tank and at the heat exchanger have been reviewed to see if the built-in conservatism is sufficient in the light of measured distributions. It appears that although the leakage from the neutron shield may be greater than anticipated, the softer spectrum means that fluxes at the heat exchanger may not be correspondingly high. At worst a factor of two increase in the maximum activity of secondary sodium is calculated. No excessive radiation levels would result.

## 5. Instrumentation and Control

a. Preparation for Wet Critical Experiments - Minor corrections and revisions to the instrumentation and the control system are being made as the need becomes apparent during preparations for wet critical experiments. For dry critical experiments the nuclear instrumentation was of greatest concern and therefore received the most attention. During wet critical operation, temperature, level, pressure, and flow measurements for the sodium system will play an important role and a detailed review and checkout of this equipment is being made.

Temporary revisions such as temperature recorder range changes and installation of extra thermocouples on various components are being made for the high temperature test on the primary tank.

One substantial change being made in the control system provides for completely manual (not electrical) operation of the safety rod drives for their withdrawal to the "remove" position. There they may be replaced. Appropriate control system interlocking will be designed to accommodate this manual operation and provide for its effective administrative control from the control room.

The circuitry previously used to bypass the period scram in the counting rate channels when the flux level was too low to provide a satisfactory period signal is being converted for use as a low flux level startup interlock. In this application it prevents startup if the source flux level is below a safe value.

b. Fuel Element Failure Detector - The fast fourfold coincidence circuit described in the last Progress Report has been put into service after some modifications which were found to be necessary in the course of extensive testing. At the same time, the "gate timing" circuit, which was developed previously and has been used for some time, was simplified and adjusted to feed pulses of the right shape and amplitude to the new coincidence unit. The prototype fission counter is assembled and ready for filling. The first of two amplifiers is ready, now that several small defects have been eliminated. The loop on which this equipment is to be located at EBR-II is now being designed.

c. Automatic Control System - A revision was begun to a digital program for the computation of control rod switch points from the analytical solution to the kinetics equations with feedback. The new program will allow the problem parameters to be changed more easily, thus facilitating a parameter study and a comparison of results with a revision to the kinetics equation code, RE-129.

## 6. Fuel Cycle Facility

The Fuel Cycle Facility is only slightly more than 98 percent completed. Progress in finishing work continues to be slow since most of the manpower has been assigned by the contractor to corrective work.

The removal of corrosion pits (see Progress Report for November, 1961, ANL-6473) from the flanges on the service sleeves in the Argon Cell is continuing.

The 31 shielding window tank units have been corrected, and the units are being prepared for reshipment to the EBR-II site.

Drawings for the installation of an emergency diesel generator in the Fuel Cycle Facility have been made. The generator will power critical items in the Fuel Cycle Facility in the event of power failure at the EBR-II site.

An order has been placed for a pillar jib crane. The crane will have a 5-ton capacity and will be used to move material in and out of the Argon and Air Cells through the shielded roof hatches.

Additional experiments were performed to investigate the use of Pittsburgh Plate Glass Company's No. 6788 glass for gamma dosimetry. This is the Company's regular 3.3-density lead shielding glass with the cerium oxide content reduced from about 1.85 to about 0.85 weight percent. The glass has met the requirements of economy, stability, and reproducibility, and has absorption properties which permit it to be used in the form of relatively thick samples. The dosimeters will be used to measure the gamma dosages received by process equipment in the Argon and Air Cells of the Fuel Cycle Facility. The radiation intensity within the cells is expected to vary between  $10^4$  and  $10^6$  rad/hr in the areas of interest. In this intensity range, the integrated dosimeter readings are found to be virtually independent of the rate of exposure. An empirical relation was found between a quantity  $\Delta T_{a,b}$  and gamma exposure of the glass. The quantity  $\Delta T_{a,b}$  is defined by the equation

$$\Delta T_{a,b} = T_{500} - T_{425}$$

where  $T_{500}$  and  $T_{425}$  are the transmittancies of the samples at the wavelengths shown. The empirical relationship between  $\Delta T_{a,b}$  and the gamma exposure is

$$\Delta T_{a,b} = -0.126 + 0.03 \log_{10} E$$

where  $E$  is the gamma exposure in rads. The maximum error in the determination of the gamma exposure was found to be 20 percent.

Resistors were installed in all the dynamic braking circuits in the mockup control cabinets. Braking action is now less abrupt. Similar resistors have been ordered for installation in all control cabinets for the manipulators at the EBR-II site.

Testing of the ingot remover and sampler is nearly completed. This equipment is used to remove the melt refined ingot from the graphite mold and to remove a protrusion from the bottom of the ingot. The protrusion serves as an analytical sample. No difficulties were encountered in the operation of the equipment.

The transfer of liquid magnesium, zinc, and cadmium between two containers through a heated tube is being studied. Several successful transfers have been made with cadmium. An attempt to transfer magnesium vapors with argon gas as a carrier was unsuccessful as a result of a stoppage in the transfer line. Examination of the line revealed that the stoppage occurred at the flanges which acted as heat sinks. The dismantled tube and flanges are being reworked to cut heat losses.

## 7. Process Development

a. Melt Refining Process Technology - Some additional information has been obtained on the volatilization of condensable fission products during the melt refining of highly irradiated EBR-II prototype fuel pins. Analyses of activities collected on nickel specimens suspended in the melt refining enclosure indicated that the fission products were volatilized in the following decreasing order: cesium > iodine > alkaline earth metals. Smaller amounts of rare earths, zirconium, tellurium, and ruthenium activities were also present on the specimens.

Additional experiments were conducted on the nitridation rates of irradiated uranium-fission pins in a nitrogen atmosphere. The rate of nitridation appeared to be more dependent on the extent of surface roughening and swelling of the pins during irradiation than on the specific activity present.

During the nitridation studies, a volatile substance was collected as a waxy deposit in a portion of the apparatus. It is likely that the source of this material is butyl alcohol which was used to remove NaK from the pins. It is believed that the butyl alcohol undergoes a radiation-induced reaction in which higher-boiling organic compounds are formed. Since butyl alcohol was used to remove NaK from the fuel pins in the melt refining runs with highly irradiated fuel, it now appears possible that some carbonaceous material was present during the runs. A reaction between zirconium and the organic material would explain the removals (10 to 20 percent) of zirconium that were obtained in the melt refining experiments.

b. Skull Reclamation Process - Adequate purification of uranium continues to be shown in demonstration runs of the skull reclamation process. In the latest run, 82 percent of the uranium in the initial charge was recovered as the purified product. Nine percent of the uranium remained as heels in the crucibles used for the reduction step and the retorting step, and 4.6 percent was found in the waste streams. About 4 percent remained unaccounted for. The principal losses occurred in the supernatant solutions of the two precipitation steps. To reduce these losses, it is planned to cool the mixture further before separating the supernatant solutions.

Pressed-and-sintered beryllia crucibles continue to show promise for retorting the uranium product. In recent runs, the yields of easily removable, agglomerated uranium product have been greater than 99 percent. A retorting experiment was also carried out in a flame-sprayed-and-sintered tungsten crucible. The uranium product adhered firmly to the tungsten crucible. In two previous experiments with tungsten crucibles yields of 83 and 98.4 percent of uranium product were obtained. The inconsistency of these results requires that further studies be made before the suitability of tungsten crucibles for the last three steps of the skull reclamation process can be judged.

c. Blanket Processing - In blanket process work, attention is being directed to the isolation of plutonium from a 50 weight percent magnesium-zinc solution. Evaporation of the solvent appears to be the most straightforward procedure, but the possibility of isolating the plutonium as a compound, which could be decomposed later, is also being considered. In a preliminary experiment, about 75 percent of the plutonium was precipitated from the magnesium-zinc solution as the hydride. The initial solution contained 0.1 percent plutonium and 0.024 percent uranium (approximately the uranium saturation concentration).

d. Reduction of Thorium Dioxide - Complete reductions of thorium dioxide to thorium metal by 5 weight percent magnesium-zinc solutions in the presence of a calcium chloride-magnesium chloride-calcium fluoride flux have been achieved in three hours. The optimum calcium fluoride concentration in the flux appears to be about 7 mole percent.

e. Materials and Equipment Evaluation - Materials studies are in progress to evaluate the compatibility of various materials with liquid metal-fused salt systems of the types contemplated for reprocessing nuclear reactor fuels. Additional solution stability runs have shown that uranium-magnesium-zinc solutions are very stable in tungsten crucibles. Because of this and the inertness of tungsten to corrosion by the magnesium-zinc-fused salt systems, tungsten is considered a desirable material for the fabrication of crucibles. Methods of fabricating tungsten crucibles are being considered. Two of the most promising methods are (1) isostatically pressing tungsten powder followed by sintering and (2) plasma-arc spraying

of tungsten powder on a mandrel followed by sintering. The fabrication of tungsten accessories, such as agitators, is also being studied. Vapor-deposited tungsten coatings applied to stainless steel, molybdenum, tantalum, Pyroceram, mullite, and graphite base materials were tested by thermal cycling between 800° and 100°C. All coatings flaked or peeled with the exception of that on graphite.

An argon-filled dry box to be used as a welding facility has been placed in operation. The unit, which contains automatic welding equipment, is equipped with a purification system (molecular sieves, dryer, and tantalum sponge getter) through which the argon is recirculated. No difficulties have been encountered in the first 200 hours of operation.

f. Preparation of Fast Reactor Fuels - An attempt was made to coprecipitate plutonium and uranium as carbides from a 20 percent magnesium-zinc solution through reaction of dissolved uranium and plutonium with finely divided carbon. Although the uranium was essentially completely precipitated, only about one-fifth of the plutonium was precipitated. Further attempts were made to precipitate the plutonium as the carbide by increasing the magnesium concentration successively to 40 and 60 percent. At these concentrations, the amount of plutonium precipitated increased to 64 and 75 percent, respectively. It should be noted that in previous experiments complete reaction of plutonium with carbon was obtained in pure magnesium solutions.

### III. REACTOR SAFETY (040117)

#### A. Thermal Reactor Safety Studies

##### 1. Fuel-Coolant Chemical Reactions

The series of condenser discharge runs with aluminum wires is continuing. The runs are being made in water at 200°C. Previous studies in room temperature water failed because the wires did not heat uniformly. Wires broke in a few places and the discharge energy was dissipated as arcs. Preliminary results in 200°C water indicate that the wires are heating uniformly and that useful data will be obtained.

Further studies of the reaction of aluminum-uranium alloys with steam have been made by the pressure-pulse method. The presence of uranium appears to increase the reaction rate somewhat. In general, the greater the uranium concentration, the faster the rate. No sudden increase occurred up to 40 w/o uranium at 1200°C.

Construction of apparatus for the study of metal-steam reactions by the levitation melting method is nearly completed. The flowing steam apparatus and the Pyrex, high-vacuum, gas-handling system for the determination of hydrogen generated by reaction have been completed.

Four transients in TREAT were completed on graphite fuel specimens. This is a cooperative program with Westinghouse which is being carried out at Argonne. Data on the peak temperature attained by the fuel specimen as a function of the energy of the reactor burst indicated that the heating process was nearly adiabatic up to 1500°C. At higher energy inputs (up to 2580°C fuel temperature recorded with a tungsten-rhenium thermocouple), the peak observed temperature was considerably less than that calculated for adiabatic heating, thus indicating that there was appreciable heat loss.

##### 2. Metal Oxidation and Ignition Kinetics

Determinations of the isothermal oxidation rates of uranium over the temperature range 300° to 600°C are continuing. Several runs were performed using a constant volume and following the pressure decrease with a strain gage pressure transducer. Accurate results were obtained during the first minute of reaction in this way. Results obtained by the slower responding volumetric procedure were confirmed.

A series of calculations of the burning temperatures of metals in air were initiated. The method assumes that there are no chemical barriers to oxidation. Reaction rate is controlled by the gaseous diffusion



of oxygen through a boundary layer of nitrogen surrounding the burning metal. Calculations have been completed for the case of natural convection to a vertical plate (foils), to a horizontal cylinder (wires), and to a sphere. Precise values for particular cases depend on a knowledge of the emissivity of the oxidizing metal surface. Reasonable values exist for zirconium; however, little or no uranium data could be found. For this reason, an experimental program was started to measure the emissivity of oxidized uranium.

X-ray diffraction examination of uranium cubes after extensive oxidation at 400°, 500°, and 600°C has shown the presence of progressively higher oxides on the cube face proceeding from  $\text{UO}_2 + \text{U}_3\text{O}_7$ ,  $\text{UO}_2 + \text{U}_3\text{O}_7 + \text{U}_3\text{O}_8$ , to  $\text{U}_3\text{O}_8$  at 600°C.

Because of the effectiveness of Freon 152 ( $\text{CH}_3\text{CHF}_2$ ) in limiting uranium combustion, it was hoped that some means could be found to reduce the hazard of flammability of the organic compound itself. A device has been constructed for examining the flammability limits of gases and several preliminary tests have been made. The lower limit of flammability of Freon 152 reported by DuPont (5 percent) has been confirmed. It is planned first to examine the effect of  $\text{CF}_3\text{Br}$  on flammability limits of  $\text{CH}_3\text{CHF}_2$  and then to explore the effectiveness of suitable nonflammable mixtures of these two compounds on uranium combustion.

The spherical zirconium powder being used for powder ignition studies was found to contain aggregates of fine particles. These aggregates were broken up and separated into proper fractions by a combination of shaking on the Wig-L-Bug without an impactor and subsequently sieving in the presence of ionizing alpha radiation. The program of study of ignition parameters will continue.

Plutonium ignition experiments have been performed with the burning curve method using 0.5-cm cubes. Samples containing 0.5 and 1 atom percent silicon ignited approximately 40 degrees higher than similar samples of alpha plutonium.

## B. Fast Reactor Safety Studies

### 1. TREAT Program

In-pile experiments are being continued in TREAT on fast reactor fuel samples to obtain information on the types of fuel element failure, meltdown product movement, and the associated mechanisms producing such phenomena.



a. Dry Transparent Experiments - Five samples of argon-bonded uranium oxide fuel elements were exposed in TREAT transparent capsules. All samples were of 10.9% enrichment and 92% theoretical density uranium oxide cylinders, 0.180 cu in. diameter, and clad in EBR-II type fuel jackets. The cladding of three of the samples was of stainless steel, and the remaining two samples were clad in tantalum. These were the first meltdown tests on prototype fast reactor oxide fuels in transparent assemblies which permit photographing of the samples during irradiation. The experimental conditions are summarized in Table VIII.

Table VIII. Series XXVIII, First Transparent Meltdown  
Uranium Oxide, EBR-II Type Fuel Elements

<u>Transient</u> <u>No.</u>	<u>Sample</u> <u>No.</u>	<u>Cladding</u>	<u>Total</u> <u>Integrated</u> <u>Power</u> <u>(Mws)</u>	<u>Maximum</u> <u>Recorded</u> <u>Cladding</u> <u>Temperature</u> <u>(°C)</u>
1	1	Steel	85	1275
2	2	Steel	146	Melt
3	3	Steel	183	Melt
4	4	Ta	132	~1700(1)
5	4	Ta	132	~1700(1)
6	4	Ta	136	-(2)
7(3)	5	Ta	-	-

(1) Limit of reliability of Pt/Pt-10% Rh thermocouples.

(2) Thermocouples lost in Transient Nos. 4 and 5.

(3) Records not yet received.

The samples have been shipped to the Argonne, Illinois site for post-mortem examination.

Metallographs have been made on oxide samples which were exposed in TREAT during Series XXV and Series XXIV. These metallographs showed extensive cracking throughout, reflecting the high degree of thermal shock suffered by these samples. These results will be compared with those obtained from examination of samples exposed in Series XXVIII.

b. Remote Capsule Assembly - The cask designed to handle the capsules for the exposure of pre-irradiated elements has been received. The unit is now being assembled and will be tested by drawing a sample of CP-5 fuel element into the cavity while external activity readings are taken.

The remote closure welding of the capsule has been successfully accomplished and test welds were made. Sectioning and polishing of these welds have shown that the closures are very uniform.

A total of twelve of the twenty EBR-II elements irradiated in the MTR have been removed from their capsules and have been examined. None of these samples have suffered damage or destruction in any way. The estimated burnups range from 0.52 to 1.18%. Activity measurements made upon these samples show readings ranging from 125R at 2 in. to 500R at 3 in. taken at the midplane of the fuel element axis.

c. Stagnant Sodium Capsule Tests - Two of the four stagnant sodium capsules in Series XXVII were received and examined during this period. This group of tests comprises a study of the effect of an axially-shaped neutron flux on the failure of 3% enriched EBR-II fissium prototype fuel elements immersed in stagnant sodium. Experimental conditions are summarized in Table IX.

Table IX. Series XXVII, 3% Enriched Fissium Alloy,  
EBR-II Fuel Elements in Stagnant Sodium

Sample No.	k <sub>ex</sub> (%)	Total Integrated Power (Mws)	Maximum Recorded Temperature (°C) <sup>(1)</sup>
1	1.54	152	680
2	1.52	197	730

(1) Thermocouple imbedded in end of fuel pin, in region of tantalum neutron absorber.

Neither of the two samples failed by penetration of cladding during the transient. Sample No. 1 was slightly warped, and its helical separator wire was loose. The sodium thermal bond within the cladding was intact, with only a small spot of eutectic about one-third fuel pin length from the top of the element.

Sample No. 2 had an external appearance similar to No. 1. However, the central portion of the fuel pin was found to be considerably eroded, and covered with eutectic. The behavior of the two samples is consistent with other observations, and the coolant effect of the annular stagnant sodium is seemingly demonstrated.

Samples Nos. 3 and 4 of this series are under preparation and should be shipped to TREAT soon. Since the first two tests of the series

yielded results indicating the reactor energy release was about 16% lower than needed to obtain extensive failure of the fuel samples, tests 3 and 4 will be initiated with higher  $k_{ex}$  and clipped at a higher total integrated power.

d. Small Sodium Loop - Several difficulties have been encountered in the testing of the small sodium loops. The first resulted from the unexpected appearance of a leak in the electro-magnetic pump tube at the electrode-to-tube transition weld seam. It was subsequently determined that this was caused by cracking of the metal under the stresses produced by welding. This recurrent condition necessitates microscopic examination of all pump tubes before installing them in pump assemblies.

The second problem is concerned with the inexplicable loss of sensitivity of the pressure transducers when sodium is introduced into the loop. Good results have been obtained from prior pressure calibrations of the transducers, at temperatures up to 375°C, using gas pressure. However, when molten sodium was the fluid medium, the strain-bridge transducers became inoperative. The problem is under investigation.

The cask design has been started, in conjunction with a preliminary study of the required handling sequence for the experimental assembly. A study of the instrumentation requirements has been completed, and circuitry drawings are in preparation. Instrument types have been selected.

e. Large Sodium Loop - The final building conversion requirements have been set for the pit, stairs, and equipment crane in the TREAT building.

Remote handling procedures have been studied and discussed with the Remote Control Division personnel. In addition, the preliminary cask design was discussed with Special Materials Personnel, and was declared acceptable. Calculations for the final cask design have been completed.

The sizing and location of the loop heaters is underway, and it is expected that this aspect of the loop design will be completed shortly. The system will require 80 kw of power for thawing and heating to a temperature of 480°C in 5 hours. The sodium compartment cooling requirement of 25 kw (7 tons) can be satisfied most compactly and economically by forced air evaporative cooling.

## 2. Theoretical Studies

a. Heat Transfer Calculations for Fast Reactor Elements in Liquid Metal Coolants - In a previous progress report (ANL-6473, Reactor Development Program Progress Report, November 1961), mention was made of a study of the axial variation in heat transfer coefficient from a cylindrical pin in an idealized model of a possible TREAT meltdown experiment. The model considered was that of a heated EBR-II fuel element surrounded by a cluster of unheated EBR-II elements on the EBR-II pitch.

One of the conclusions drawn from the study was that satisfactory results should obtain if the available turbulent flow correlations were used to predict sample heat fluxes over the entire length of the fuel element.

A further study has been made of the available correlations for fully developed turbulent heat transfer coefficients, for parallel flow through a bundle of fuel pins. Of the theoretical correlations available, four were considered to be most applicable to the meltdown model hypothesized previously. It was concluded that none of the four correlations would correctly predict heat transfer coefficients for fully developed turbulent flow of sodium through a bundle of pins having a pitch-to-diameter ratio of 1.28. These predictions are consistently much lower than the values obtained in the small amount of experimental work performed, and this is to be expected for the particular case of parallel flow through a bundle of pins.

In the absence of a more exact correlation, and with an estimate of the discrepancy between available correlations and the modelled meltdown case, it is suggested that Nusselt numbers in fully developed turbulent flow may be calculated by increasing the values in the relation due to Seban by 20%. The revised equation would be

$$Nu = 6.96 + 0.024 Pe^{0.8} \quad ,$$

It was also concluded that a study should be made to determine the temperature variation around the circumference of the pin. In all the available analyses of correlations of turbulent heat transfer coefficients, the circumferential temperature variation has been neglected. However, it has been demonstrated that appreciable circumferential temperature gradients exist in a fast reactor fuel assembly, especially where the fuel pins are wrapped with helically pitched wire, which further increases the irregularity of the coolant passage shape. If the circumferential temperature gradients are appreciable in the meltdown experiments, their presence might determine the angular position of a fuel pin failure.

#### IV. NUCLEAR TECHNOLOGY AND GENERAL SUPPORT (040400)

##### A. Applied Nuclear Physics

##### 1. 3.0 Mev Van de Graaff

a. Fast Neutron Scattering by Time-of-Flight - During the past month approximately one hundred hours of accelerator time were devoted to studies of the angular distribution of elastically and inelastically scattered neutrons from  $U^{238}$ ,  $U^{235}$ , tungsten, and tantalum. The incident energy extended from 350 kev to 1.2 Mev. The  $U^{238}$  results are a continuation of those recently shown (ANL-6473, Monthly Progress Report for November 1961). The studies of elastic scattering from tantalum are summarized in Figure 4. In addition to the elastically scattered component given in the figure, the differential cross section for inelastic scattering from tantalum was obtained throughout the incident neutron energy range. For each of the studied isotopes, the measured inelastic and elastic differential scattering cross sections are in good agreement with the published total scattering cross sections.

A very encouraging aspect of the above work is the steadily increasing precision of the measurements and the reliability of the sensitive apparatus employed. Continuing improvement in both data processing and automation of the equipment has increased the experimental productivity.

b. Fission Fragment Mass and Angular Distributions - Ignoring neutron and gamma-ray emission, it can be shown that

$$\frac{M_1}{M_1 + M_2} = \frac{E_2}{E_1 + E_2} = \frac{V_2}{V_1 + V_2}$$

where  $M_1$  and  $M_2$  are the fission fragment masses,  $E_1$  and  $E_2$  are their respective energies, and  $V_1$  and  $V_2$  are the corresponding voltage pulses produced from linear detectors. The pulses are added and the indicated division is performed electronically. Initial tests using diffuse junction solid state detectors and 100 mg of  $U^{235}$  mounted on an 80 mg nickel foil gave a peak to valley ratio of about 200 when all of the fission events were accepted and a ratio of about 550 when only those fissions with a total energy greater than 160 Mev (about 60%) were accepted. These values must be compared to the peak to valley ratio of about 600 obtained by radiochemical methods. The low peak to valley ratio obtained when all fissions are accepted may be in part due to "windows" and non-linearities in the detectors and to small fission pulses obtained when the fragments enter the edges of the detectors.

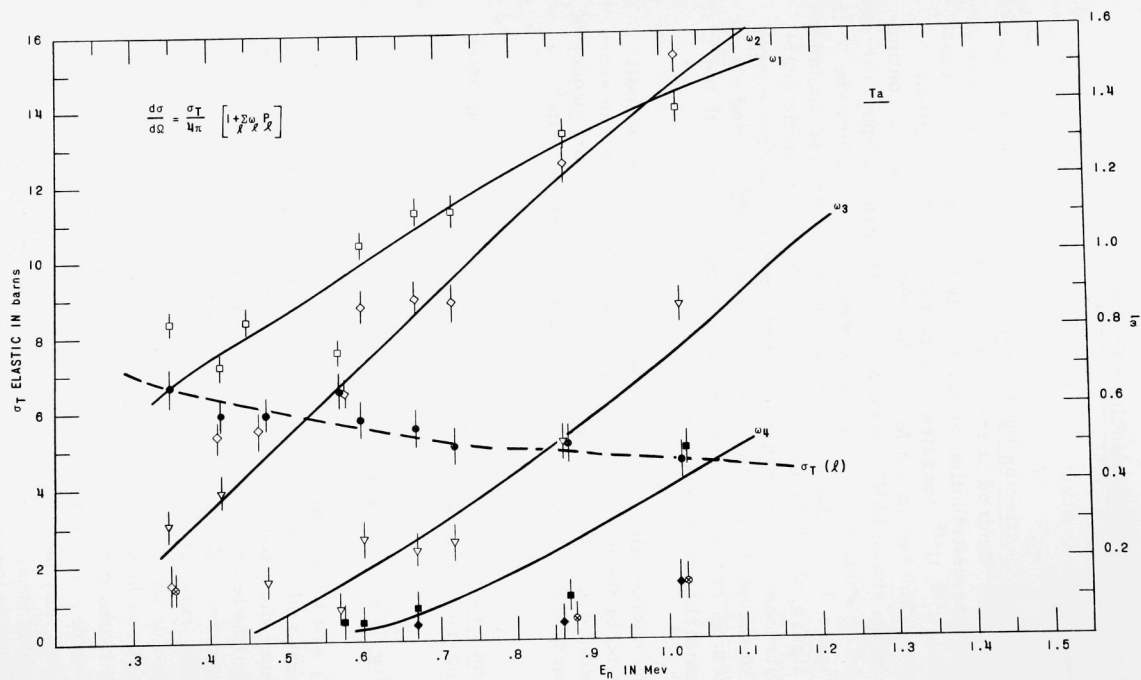


Figure 4

Elastic Scattering of Neutrons by Tantalum

Some measurements have been made of the effect of bias voltage on the response of the diffuse junction detectors to fission fragments. For detectors fabricated from about 1000 ohm/cm material, variation of the bias voltage over the range 1 to 100 volts gave no change in the relative heights of the light and heavy mass peaks. The dependence of the pulse rise time over the same bias voltage range is given by

$$\tau = 170 V^{-0.54} .$$

Rise times for alpha particles are  $\leq 10$  nanoseconds.

c. Neutron Capture Cross Sections - The absolute neutron capture cross sections of  $\text{Rh}^{103} (n, \gamma) \text{Rh}^{104m}$  and  $\text{Rh}^{103} (n, \gamma) \text{Rh}^{104}$  were measured using activation techniques. Cross sections for the 4.4-min activity ( $\text{Rh}^{104m}$ ) and the 42-sec activity ( $\text{Rh}^{104}$ ) were obtained independently. Two counting methods were used for the cross section determination. In the first method thin (about 2-8 microns thick) rhodium foils were irradiated in a known neutron flux measured with a  $\text{U}^{235}$  fission chamber, and then counted in a  $4\pi$  space beta counter. In the second method, the beta activity from a thick (250 micron) rhodium foil was compared to the fission rate from a  $\text{U}^{235}$  foil in a fast (500 kev) neutron flux and a thermal neutron flux.

The results for the capture cross section leading to the 4.4-min activity of  $\text{Rh}^{104m}$  and the 42-sec activity of  $\text{Rh}^{104}$  are given in Table X. The error in the cross section values has not been fully evaluated; however, a tentative error of  $\pm 20\%$  is placed on all measurements.

Table X. Capture Cross Sections of  $\text{Rh}^{104m}$  and  $\text{Rh}^{104}$

$E_n(\text{kev})$	$\text{Rh}^{104m}$	$\text{Rh}^{104}$
	$\sigma_c(42 \text{ sec}) \text{ barns}$	$\sigma_c(4.4 \text{ min}) \text{ barns}$
175	.329	.041
200	.295	.040
250	.232	.033
300	.227	.032
350	.210	.026
400	.0148	.022
450	.127	.018
500	.094	.014
600	.092	.013
700	.073	.012
800	.053	.011
900	.056	.009
1000	.056	.010
1100	.050	.009
1200	.042	.010
1300	.044	.009
1400	.037	-
1500	.038	.009
1600	.034	.009
1700	.031	.009

## 2. Argonne Thermal Source Reactor (ATSR)

a. Resonance Integral Measurements - Measurements were made to allow an estimate of the reactivity contributions due to scattering and slowing down by foil samples. Observations of the reactivity effects of carbon and teflon when oscillated in the cadmium tube indicate that the effects are due almost entirely to slowing down of neutrons and subsequent capture in the cadmium. The reactivity effects appear to be proportional to  $\xi \Sigma_S$ . Oscillation of a lead sample seems to indicate that effects due to scattering of neutrons out of the tube are negligible.

Calibration of the resonance integral measuring system was begun. After several days of observation it became apparent that the rod response was nonlinear. Study of the various possible causes is still in progress. The rod drive system has been overhauled and improved, and all mechanical difficulties seem to have been overcome.

During a routine check of the reactor system it was determined that the reactor core water had become somewhat radioactive. The reactor was out of operation for approximately a week and a half during which time the core water was replaced, the core tank rinsed, and the 2 x 6 x 0.025-in. uranium-aluminum alloy fuel plates replaced with plates having a protective coating of "Heat-Rem" aluminum paint.

b. Flux Perturbation Measurements - Activation and counting of a first series of gold foils in a graphite block driven by ATSR was completed. The foils were activated in the center of a 20-cm cubic void in the graphite block. The cadmium ratio at this location was between 400 and 900 depending on the thickness of the foil. The foil thicknesses ranged from 0.00075 to 0.05 cm. Foils of eight different thicknesses within these limits were irradiated with both aluminum and cadmium covers. The intensity of each irradiation was monitored by a foil located in the graphite 30 cm from the reactor interface. This monitor foil was cadmium covered in order to reduce its high activity. The counting rate of foils with a thickness of more than 0.0025 cm had to be corrected for gamma absorption in the foil. The correction factor was established by counting foils while they were covered by layers of different thicknesses of nonactivated gold.

The results of these first measurements gave a rough confirmation of a  $\frac{1}{2} - E_3(t\Sigma_a)$  dependence of the self shielding for incident thermal neutrons. The cadmium-covered foils which are activated mostly by resonance neutrons showed a self shielding which is not in disagreement with the formula given by Blosser, et al., in ORNL-2842. Statistical and other inaccuracies are so large, however, that the results cannot be called a confirmation of this formula. An investigation of the reproducibility of counting rates of the same foil in our counting apparatus indicates that the biggest changes occur whenever the foil is taken out of the apparatus, then put in again and counted again.



The reproducibility of the foil-counter geometry in our counter has to be considerably improved. There are also slight shifts of counting rate with time (apart from natural decay) when the foil is not moved between counts. These may be due to voltage instabilities and are not as serious as those mentioned before.

### 3. $\bar{\nu}$ for $U^{235}$ and $Cf^{252}$

Most of the data obtained in the  $U^{235}$   $\bar{\nu}$  measurement at CP-5 have been analyzed, and some preliminary conclusions are being established. Still to be completed for the first complete staging of the experiment is the absolute calibration of the standard  $Mn^{56}$  counter. More advanced calculations must also be made.

All three of the primary experiments carried out while using the CP-5 thermal column suffered from unstable operation of a specially designed liquid counter which used Cerenkov radiation for its signals. Because of the lag involved in processing the data, this situation was not uncovered until the allocated time at the reactor had expired. For the two relative experiments (manganese/hydrogen absorption ratio and cadmium captures) this results in an error spread in excess of the purely statistical. Hence, for the absolute counting objective an unacceptable uncertainty is present.

A new liquid scintillation counter has been checked out. After intercalibrating it with the Cherenkov-NaI liquid counter, the latter will be dismantled and replaced by a more efficient and stable  $\gamma$ - $\gamma$  detector. The scintillation counter will again be used for intercalibration. The system will be checked out with a Ra- $\alpha$ -Be source prior to receipt of the required  $Cf^{252}$ . In addition, a set of concentration runs will be carried out with the Ra- $\alpha$ -Be source, to provide some useful information on the effective manganese/hydrogen absorption for hard spectrum neutrons. This quantity is critical to most neutron standardization efforts, and such direct measurements have not heretofore been made for any fast neutron source.

### 4. Fast Spectrum Measurements

The measurement of fast neutron reactor spectra has been performed in the past with moderate success by a method involving the detection of recoil protons produced by a neutron beam emanating from a fast reactor assembly (Perlow coincidence spectrometer technique). Two alternate methods which promise improvement through higher efficiency and elimination of the need for collimated neutrons are being investigated. One employs solid state detectors, the other uses electronic processing of the pulses from a gas-filled counter to distinguish the neutron-induced pulses from those caused by gamma rays.

$\text{Li}^6$  has been compared to  $\text{B}^{10}$  as indicator material for a solid state, fast neutron spectrometer. The signal derived from the tritium produced by thermal neutron bombardment of a very thin lithium layer, separated from the detector through a moderately severe collimator, has shown sufficient resolution that lithium may be considered a more promising material than boron. A code which would resolve the spectrum of the incident flux from the effects of counter resolution, center of mass motion, and the angular distribution of the reaction products is being investigated. An alternate construction of the spectrometer will use the combined signals from the tritium and alpha particle produced in the disintegration of a lithium nucleus. The equipment to make preliminary tests of the merits of this scheme is ready; the actual testing has been delayed due to the schedule of CP-5. The proposed construction of the spectrometer will differ from that used at Oak Ridge through the added feature of collimation of either the tritium only, or of both disintegration products. This is expected to produce better energy resolution at the expense of increased size and smaller efficiency of the counter combination.

Using a proportional counter filled with a mixture of 1 atm of propane and 1 atm of  $\text{N}_2$  (in order to make use of the  $\text{N}^{14}(\text{n},\text{p})\text{C}^{14}$  reaction as a calibration line), it was possible to discriminate unambiguously against  $\gamma$ -ray background down to an energy of 100 kev. At this energy  $\gamma$  conversion electrons were more numerous than proton recoil events by a factor of 10 or more. Electron events were observed in numbers comparable to proton recoils up to an energy of about 400 kev. The  $\gamma$ -n discrimination system employed has extended the useful range of the counter by a factor of four in this case.

## 5. Study of Resolving Loss Corrections for Scaler Data

Resolving loss correction factor problems are encountered in measuring flux in critical experiments. Study of various correction factors previously used indicated a fundamental similarity which can be shown by expanding the correction factors as power series of  $(n\tau)$  where  $(n)$  is the observed count rate and  $(\tau)$  is the resolving interval accompanying an isolated scaled event. The coefficients of the power series in  $(n\tau)$  are the normalizing coefficients for the various orders of sequences which fail to resolve. In each series the coefficient of the first power term is unity; that of the second power term is the normalizing coefficient for unresolved doublets; and that of the third power term is for unresolved triplets, etc. On this basis the various factors may be compared and evaluated.

If the scaling rate is defined as  $(n)$ , the corrected rate  $(N)$ , and the resolving interval for an isolated event  $(\tau)$ , the following equations are obtained:

$$N_L = \frac{n}{1 - n\tau} = n (1 + n\tau + n^2\tau^2 + n^3\tau^3 + \dots) \quad , \text{ as a lower limit}$$

$$N_U = \frac{n}{1 - N_U\tau} = n (1 + n\tau + 2n^2\tau^2 + 3n^3\tau^3 + \dots) \quad , \text{ as an upper limit}$$

$$N_P = n^{-N_P\tau} = n (1 + n\tau + \frac{3}{2}n^2\tau^2 + \frac{8}{3}n^3\tau^3 + \dots)$$

The expression for ( $N_L$ ) implies that every scaled event is accompanied by a resolving interval ( $\tau$ ) and that unresolved events (doublets and triplets) do not extend this interval. Consequently, the normalizing coefficients are all unity and the same resolving interval is credited for unresolved doublets and triplets as for single scaled events. The expression for ( $N_U$ ) implies that scaled and unresolved events both add equally to the unresolved interval, consequently the normalizing coefficient for an unresolved doublet is two, etc. The expression for ( $N_P$ ), the Poisson formula, implies that equal intervals ( $\tau$ ) are initiated by each event whether scaled or unresolved. Since an unresolved event is just as likely to fall early as late in the interval ( $\tau$ ) following the preceding event, the intervals overlap and fractional normalizing coefficients are obtained for doublets and triplets. These fractional coefficients are the statistically averaged values for random ordered events.

Since scaling produces a count(s) during a counting interval ( $t$ ), of a foil with a decay constant ( $\lambda$ ), it may be more convenient to use these terms in treating data, as shown in the following equation. This yields a count(s) which is corrected for resolving loss.

$$S_P = s \left[ 1 + \frac{s\tau}{t} \left( 1 + \frac{\lambda^2 t^2}{12} - \epsilon_1 \right) + \frac{3}{2} \frac{s^2 \tau^2}{t^2} \left( 1 + \frac{\lambda^2 \tau^2}{12} - \epsilon_2 \right)^2 + \dots \right]$$

The corrected count equation is equivalent to the count-rate equation if ( $\lambda t$ ) is small. The ( $\epsilon_1$ ) terms are almost inconsequential for a counting interval shorter than a half-life. They may be as large as ( $1/100$ ) if ( $\lambda t$ ) exceeds unity.

## 6. High Conversion Critical Experiment

Experimentation continued with the 1.27 cm pitch triangular lattice BORAX-V fueled core. Measurements included thermal utilization, fast fission factor, and  $U^{238}$  capture cadmium ratio. Neutron temperature plus supplementary measurements at resonance energies are being made. Close agreement was obtained in measuring the central void coefficient by water displacement using aluminum void tubes and teflon rods. The coefficient is - 0.6% reactivity per % void.

## 7. Theoretical Reactor Physics

a. Transport Approximations in Thermal Reactor Lattices - The simplified integral transport approximation employed in slab geometry heterogeneity calculations<sup>1</sup> of fast critical assemblies has been applied to a sample problem of thermal reactor lattice self shielding. The periodic slab lattice has nonscattering absorber of thickness 0.295 mean free paths, and non-absorbing moderator of thickness 9.1504 mean free paths. A ratio of  $\bar{\phi}_{\text{absorber}}$  to  $\bar{\phi}_{\text{moderator}}$  of 0.802 is obtained. By a single flat-source iteration the value becomes 0.789. These may be compared with the "exact" value of 0.7843 reported by Bohl, *et al.*<sup>2</sup>

b. Fuel Cycle Studies - The IBM-704 fuel cycle program CYCLE has been used to analyze 175, 350, and 700 Mwe plutonium-fueled fast reactors for representative metal, oxide, and carbide systems. The following assumptions were made: 1 Mw/liter power density in the core for the metal and carbide systems and 0.5 Mw/liter for the oxide systems; a thermal efficiency of 0.4 for the oxides and carbides and 0.35 for metal. The metal systems had a 2% burnup in the core and a 0.5% fission product buildup in the innermost blanket region. The oxides and carbides were allowed to burn to 5% in the core and 1.25% in the innermost blanket zones. All systems utilized cyclic core and blanket management schemes.

Examination of the breeding gains attained in the various blanket zones indicate that the 40 cm used for the metal blankets is probably a reasonable thickness but that the original 60-cm oxide and 50-cm carbide blankets should be reduced to 50 and 45 cm respectively. Subsequent problems will also incorporate an outer 10-cm inert reflector of 90% stainless steel and 10% sodium.

Cost analyses on these first nine problems indicate that fabrication and processing costs represent a major fraction of the total core and blanket fuel costs. In addition, for the assumed basic charges, the carbide systems had consistently the lowest costs and the metal systems the highest.

Work is currently being done to improve the nuclear cross sections of the light elements with the help of the ELMOE code. In addition, lower values as given by the latest experimental data will be used for  $\nu$  of  $U^{235}$  in further CYCLE problems.

---

<sup>1</sup> D. Meneghetti, "Convergence of Transport Solutions for Thin Slab Cells," ANL-6345 (April 1961).

<sup>2</sup> L. S. Bohl, J. C. Stewart, and N. C. Francis, Nuc. Sci. & Eng. 4, 257 (1958).

## 8. Mathematical Numerical Methods Analysis

A major source of difficulty in communicating computational schemes by publication in a problem-oriented language is the difficulty of eliminating human errors in typing, typesetting, and card punching. To reduce these errors, redundant information, such as parity and sum checks can be introduced, and published along with the procedure. Unfortunately, the typical algorithm is quite a specialized type of message, with a non-random, and so far unknown distribution of symbols, and the errors which may be expected are far from the simple distributions treated in standard information theory. An ad hoc scheme must therefore be devised.

For checking algorithms written in Algol, the following criteria seem desirable:

(1) The scheme should be compatible with the structure of Algol 60. Programs and sub-programs containing the checking data should be translatable on any translator which could translate the program alone.

(2) The check should cover not only the entire program, but its logical subdivisions, so that installations desiring to use only a part of a published program, or wishing to modify it in certain respects, need not lose all checking capability. The effects of changes in the program should be as localized as possible.

(3) Error detection should be emphasized. Although automatic error correction is not believed worthwhile, error indications should, as far as convenient, assist human isolation and correction of the errors. Errors of types expected to be particularly likely, such as transpositions of symbols, words, or even whole lines, should be detected with high efficiency.

(4) Minimization of redundancy, though desirable, is subordinate to the preceding three goals.

A scheme for generating and inserting check data of this type into Algol programs has been developed, programmed for the LGP-30 computer, and tested on a few samples. It was found to detect errors satisfactorily with approximately 18% redundancy. Study of the results indicated that the redundancy could be reduced by almost two-thirds with little loss in power. A program for the revised version has been written and is being tested.

## B. Reactor Fuels Development

### 1. Corrosion Studies

a. Aluminum Powder Tubing in Corrosion Testing - Armour Research Foundation has supplied about 60 ft of two new batches of powder product tubing (Alloy A288 - 1 w/o Ni, 0.5 w/o Fe, 0.1 w/o Ti): one made from the as-atomized alloy powder and the other made from powder that had been ball milled 48 hours. A short test at 350°C in water indicated no catastrophic failure for either type of tubing. A longer more carefully controlled test has been started at 290°C, the temperature of maximum attack for most low silicon aluminum powder products. Accelerated edge corrosion, typical of previously tested tubing, requires from 60 to 100 days before it is apparent, so the new tubing cannot be evaluated until after that period of time.

An Alcoa powder product tube from an old batch was vacuum heat treated (550°C - 2 hours) to remove hydrogen. Its resistance to blister attack and also to the accelerated edge corrosion mode of failure were significantly increased. Samples of the ARF tubing mentioned above have also been given this treatment before corrosion testing.

b. Zirconium Alloys for Superheated Steam - Hydrogen analyses indicate that it is possible to keep the hydrogen content relatively low in corroding zirconium alloys. For example, the Zr-1 w/o Fe-1 w/o Cu alloy absorbed less than 8% of the corrosion product hydrogen during seven days in superheated steam at 540°C and 600 psi. This is the smallest amount of hydrogen absorbed in any alloy produced to date, and this alloy had the lowest corrosion rate.

Some titanium-containing alloys (with relatively good corrosion resistance) specifically designed to have low hydrogen pickup also show low (25%) hydrogen absorption after 7 days at 540°C.

c. Lightweight Alloy for Liquid Mercury - The utilization of proper additives or inhibitors in mercury to reduce the corrosion attack on titanium is attractive because it permits using readily available lightweight materials.

Recent tests, the results of which are given in Table XI, conducted with saturated solutions of additives in mercury at 371°C in Pyrex glass capsules revealed again that zirconium is one of the most promising additives for reducing attack by mercury on titanium in a static system.

Table XI. Corrosion of Commercially Pure Titanium in Mercury at 371°C, with Additives

<u>Contact Time,</u> <u>Days</u>	<u>Additive to</u> <u>Mercury</u>	<u>Specimen Weight</u> <u>Loss, mg/cm<sup>2</sup></u>
7	None	26.20
14	Fe	1.37
14	Cu	1.09
14	Zr	0.56
14	Mg	1.43

Chemical analyses to determine concentrations of the inhibitors and the amounts of titanium dissolved in the mercury are now in progress.

## 2. Nondestructive Testing

a. Neutron Techniques - During the past month efforts have been extended toward improving understanding of the image sharpness qualities which can be obtained using various detection methods. Much of the effort was directed toward improving the equipment used for this study. The original equipment has been modified and automated to a much greater degree than previously. This is expected to result in the assembly of appreciably more data in this phase of the investigation.

The equipment now seems to be in good order and reproducible data can be obtained. One result which has come out of the early studies making use of this equipment is that, from an image sharpness point of view, gadolinium screens of 0.0005 in. and 0.001 in. thicknesses yield better neutron radiographs than do 0.002 in. screens. There is also a good indication that the use of a 0.005 in. lead intensifying screen with a thin gadolinium screen for direct exposure neutron radiography yields as good image sharpness as the gadolinium alone. The lead screen technique would be preferred because of its increased speed.

b. Radiographic Technique - Several clad plates were examined by an X-ray fluorescence technique for homogeneity. Beta radiation from a  $\text{Sr}^{90}\text{-Y}^{90}$  source was used to excite k X-rays from uranium in the core. Since calculations show that about 97% of the primary  $\beta$  radiation is absorbed in the upper layers of clad and core, it was expected that this technique would be relatively insensitive to core thickness and only measure dispersion of the  $\text{UO}_2$ . It was observed, however, that cladding thickness variations of the order of 1 mil produce variations as large as does a 2 or 3 percent change in  $\text{UO}_2$  concentration in the plate.



A method for determining the total weight of  $U^{235}$  in CP-5 fuel tubes is being developed. A standard was prepared by wrapping 16 enriched uranium foils of known  $U^{235}$  content along a cardboard tube with aluminum foil. An intermediate diameter enriched tube No. E-1 has been used in this development. Fabrication data gives the  $U^{235}$  content as 75.60 grams. However, the best results obtained to date indicate it to be 74.84 grams. The technique is being examined for systematic errors to determine if the difference from production data is real.

c. Eddy Current Techniques - Development work has continued on the pulsed-field reflection system. This electromagnetic test method replaces the sinusoidal currents and test coils or probes of our older eddy current test system with pulsed fields emanating from small apertures in special masks. Test information about the metallic specimen being examined is received as a series of reflections from the surface and from inside the metal. This system represents a possible new approach to the problem of the electromagnetic testing field.

The pulsed-field reflection system is now being used to check the sodium bond quality of plutonium-uranium-fissium alloy pins enclosed in jackets made from a variety of metals with sodium being the heat transfer agent. A number of pins were inspected with this equipment, and two were then stripped of their jackets. One showed a very serious unbonded area over practically the entire length of the pin covering about 75° of its circumference. The bond of the other pin was fairly satisfactory. The correlation of the visual inspection with the nondestructive tests was good. This test system is apparently capable of providing a very good check on sodium bond quality.

### C. Reactor Materials Development

#### 1. Radiation Damage in Steel

a. EBWR SA-212B Irradiation - Two capsules containing foil loadings identical to those which deteriorated in an EBWR test irradiation (see Progress Report, September 1961, ANL-6433, page 44) were furnace autoclaved to study the causes of failure. An examination of the capsule contents following a 1000-hr exposure at 600°F showed the same phenomena as observed in the irradiated capsule; the uranium and thorium metal foils were reduced to powders and the gold foils alloyed with cadmium. It was also observed that the cadmium jackets slumped, that the aluminum and nickel wires and capsule walls were coated with a yellow film (probably the oxide of cadmium), and that there was a heavy pitting attack on the aluminum foil holding fixture.



An examination of the contents of a second capsule after a 168-hr exposure at 500°F again revealed powdering of the uranium and thorium foils, a partial destruction of the gold by cadmium, and a heavy pitting attack of the aluminum foil holding fixture. On release of the capsule helium, the escaping gas had a foul odor similar to that of air issuing from a tire inner tube.

Chemical analyses of the products found in the capsules are in progress to establish chemical reaction mechanisms which are now a problem in elevated temperature dosimetry. Since cadmium ratios are still desired, new foil designs to contain cadmium are being prepared for additional autoclave tests.

b. Magnetic and Dynamic Properties - Shakedown operations of the FM-500 Elastomat (page 51, ANL-6473, Progress Report, November, 1961) continued during the month of December. A systematic study of geometric and environmental factors such as influence of reluctance of the magnetic path on sensitivity, vibration plane, transducer position and inter-coupling, vibration amplitude, and ambient temperature are in progress.

It has been qualitatively established that the transverse vibrations damping factor is significantly influenced by gravitational effects. The ratio of the number of vibration cycles for a  $1/e$  amplitude decay for vertical to horizontal plane excitation is about 4:5 at 6 Kcps.

c. Calculations of Radiation Damage Dose - To test the validity of the energy dependent model previously proposed<sup>1</sup> for reporting neutron exposure, irradiations are being planned in grossly different reactor spectra. Multigroup reactor theory techniques are used to calculate spectra at the locations chosen and for this purpose the model has been revised to give more detail at the high energy end. Samples of carbon steel and copper single crystals will be irradiated in the center of a CP-5 tubular fuel element, in the CP-5 core (but not surrounded by fuel), and in the fast spectrum of the EBR-I core. The steel is from original EBWR pressure vessel material. Use of copper crystals is attractive since it allows shorter irradiation times, smaller samples, and simpler testing techniques. Calculated ratios of defect production and flux rates for steel are shown in Table XII. Those for copper are comparable.

---

<sup>1</sup> A. D. Rossin, "Radiation Damage in Steel: Considerations Involving the Effect of Neutron Spectra," Nuc. Sci. & Eng. 9, No. 2, pp. 137-147 (February 1961).

Table XII. Calculated Ratios of Defect Production and Flux Rates for Steel

	Defect Production Rate*	$\phi^{**} > 3 \text{ Mev}$	$\phi^{**} > 1 \text{ Mev}$	Defects due to $\phi > 1 \text{ Mev}$
CP-5 Fueled Tube	100	1.0	5.7	52.8%
CP-5 Thimble	32	0.22	1.4	39.4%
EBR-I Core Center	27	0.52	1.96	69.3%

\*Normalized to 100

\*\*Normalized to 1

#### D. Heat Engineering and Fluid Flow

##### 1. Boiling Liquid Metal Studies

The construction of a boiling alkali metal loop is approximately 60% complete. All major instrumentation has been calibrated for use in the study of the hydrodynamic behavior of two-phase sodium flow. The loop is constructed of Type 316 stainless steel, which is limited to short-term operation at 1700°F. Recently acquired information indicates that this material is superior to other ferrous and even nickel alloys with the exception of Haynes-25, which has good mechanical and corrosive endurance up to 1850°F and short-term use to approximately 1950°F. Therefore, the boiling heat transfer loop, which will utilize the same auxiliaries as the original loop, will be constructed of either Type 316 stainless steel or Haynes-25. A refractory metal loop placed in a vacuum chamber will be designed to investigate boiling sodium above these temperatures (at higher pressures) up to burnout heat fluxes.

##### 2. Double Tube Burnout Study

The preliminary test section that had been used for debugging the experimental loop was dismantled and it was found that the inner tube had buckled and was shorting against the outer tube. It was also found that the upper electrical terminal of the inner tube had broken loose because of a very poor bond with the silver brazing material.

Two design changes have been made in the new test section now under construction: a mechanical tapered joint has been substituted for the silver brazed joint; and synthetic sapphire spacers have been utilized at the midpoint of the test section to prevent the buckling of the inner tube. Changes were made in the power control for the outer tube. Tests have shown that this change successfully eliminated the objectionable contact noise reported earlier.

### 3. Boiling from a Liquid-Liquid Interface

Experimental data have been obtained for water boiling from a mercury surface at atmospheric pressure. The results show that superheats required to initiate and sustain boiling from a liquid mercury surface are higher than those for boiling from a solid surface. Visual observations revealed that there existed favored locations for bubble formation, or nuclei, on the mercury surface. This was probably due to the fact that in spite of careful precautions to preclude the introduction of contaminants into the system a perfectly clean liquid-liquid interface could never be achieved during a run.

In an effort to explore further the process of nucleation from a liquid surface, tests are being planned using an organic liquid in place of water to investigate the effect of different physical properties. Attempts will also be made to change the surface condition of mercury by introducing solids with known surface characteristics.

### 4. Two-Phase Nozzle Tests

Tests to examine the characteristics of two-phase nozzles are being planned. These nozzles have potential uses as thermal-to-kinetic energy converters for use with magneto-hydrodynamic power generators. The initial tests will use flashing water and will measure the critical flow rate through the throat and the conversion efficiency of the nozzle. The first test nozzle has been fabricated and the loop construction for testing of the nozzle is beginning.

### 5. Hydrodynamic Instability

The analog computer program applicable to either a forced or natural circulation system has been described in the progress reports for October and November 1961 (ANL-6454 and ANL-6473). The model is now being checked against loop results at different pressures and geometries.

The latest velocity ratio correlation has been incorporated into the model. This is extremely important since the power level at which oscillations occur is dependent upon the velocity ratio correlation.

A series of tests on an unrestricted 2.38-cm ID test section is in progress in an instrumented natural circulation loop to determine the onset of instability. A preliminary test to vary sinusoidally the inlet flow to a boiling test section was successful. Frequencies of variation to two cycles per second and 10% flow were achieved. A mechanical driving system is being investigated to obtain a cost estimate for a proposed flow-to-void transfer function measurement.

## 6. Behavior of Fuel Plates in High Velocity Flow

Loop tests of a relatively short fuel box containing thin, flexible, parallel, flat plates are proposed. The fuel box would be in a holder which would allow viewing along the entire length and both the inlet and outlet ends of the fuel box. The objective would be to repeat under improved experimental conditions the visual observations obtained during the 32-mil fuel box test performed a few months ago.

These observations will be summarized. Near what was predicted as the critical divergence velocity the fuel plates began to deflect in groups of two (Figure 5A). But the plates did not actually diverge, that is,

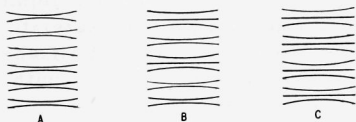


Figure 5. Behavior of Fuel Plates in High Velocity Flow

continue to deflect until they broke or obtained a permanent set by plastic flow. On the contrary, it required an increase in coolant velocity to obtain a larger deformation. Upon increasing the velocity, a quite unexpected second critical velocity was reached where the plates began to arrange themselves in groups of three (Figure 5B). At first, only one

group of three was present. Increasing the coolant velocity increased the number of groups of three until the entire box was arranged in groups of three plates (Figure 5C). The transitions occurred in wave-like motions, the plates shifting from deformations in one direction to the opposite like tumbling dominoes until a stable configuration would be obtained. By further increasing the coolant velocity a point was reached where groups of four plates were observed. At the maximum obtainable coolant velocity groups of three and four plates were observed. Lowering the coolant velocity reversed the process of plate grouping.

The purpose of the proposed test would be to determine as accurately as possible the critical velocities for various forms of plate deformation patterns for different fuel element dimensions and materials. The test then would show that fuel plate assemblies could withstand greater coolant velocities than the critical divergence velocity and do so in stable deformed patterns. The test would also attempt to verify some proposed ratios for hydraulic fuel plate deformations and provide critical values of the ratios.

## E. Separations Processes

### 1. Fluidization and Fluoride Volatility Separations Processes

a. Fluoride Separations - Irradiated uranium oxide fuels will contain mixed oxides of uranium and plutonium. A study of the removal of plutonium from mixed oxides of uranium and plutonium by reaction with fluorine is being continued. The oxides were placed in a nickel boat in a

horizontal tube furnace. Fluorine was circulated through the furnace at 800 ml/min for 10 hours; the reaction temperature was 450°C. Both alumina and nickel fluoride proved to be suitable for use as inert solids in the fluorination step in the absence of fission product elements. No increase in retention of either uranium or plutonium upon fluorination of the mixed oxides at 450°C for ten hours occurred as a result of the presence of 0.5 weight percent zirconium tetrafluoride and three weight percent nickel fluoride in Alundum. The presence of these additives resulting from fluorination of the reaction vessel or from the decladding step would not interfere with plutonium removal. About 0.5 percent aluminum fluoride was formed on the surface of Alundum by the action of fluorine for ten hours at 450°C. The use of aluminum fluoride as the inert solid resulted in retention of uranium and plutonium of 0.06 and 0.18 weight percent, respectively. This retention on aluminum fluoride is of the same order of magnitude previously found using zirconium tetrafluoride as an inert solid.

Plutonium is retained on the fluorinated Alundum which is covered with a thin layer of aluminum fluoride. Alundum residues from fluorination experiments containing varying amounts of plutonium were pyrohydrolyzed at 1000°C for two hours after which they were fluorinated for 10 hours at 450°C. About half the plutonium was removed from residues which were relatively low in plutonium, 0.04 to 0.06 percent. In order to show that this removal cannot be attributed entirely to the additional fluorination time, one portion of an Alundum residue which initially contained 0.202 percent plutonium, contained 0.170 percent plutonium after an additional ten hours of fluorination at 450°C, but another portion of the same residue contained only 0.051 percent plutonium following successive pyrohydrolysis for two hours at 1000°C and fluorination for ten hours at 450°C. This indicates that pyrohydrolysis can be utilized to limit the losses of plutonium in the Alundum discarded as waste after the fluorination procedure of the Direct Fluorination Volatility Process.

A study of the effect of fission product addition on the removal of plutonium by fluorination of the mixed oxides of uranium and plutonium contained in inert beds is now in progress. Preliminary indications are that the removal of plutonium may be more difficult in the presence of fission product oxides.

b. Direct Fluorination of Uranium Dioxide Fuel - Fluorinations of uranium dioxide pellets are being carried out at 450°C in a 3-inch diameter fluidized bed of granular Alundum. Current experiments are concerned with evaluating the effect on caking tendencies of deeper pellet beds (18 inches compared with 3- and 6-inch beds used previously). In these preliminary runs use of off-gas recycle caused severe caking probably because of excess oxygen; use of nitrogen as the fluidizing gas substantially reduced the caking but further runs are needed to find optimum conditions.

## c. Separation of Uranium from Zirconium Alloy Fuels

(1) Studies on the Hydrochlorination and Fluorination Steps with Fixed-Bed Filters - Development studies on a fluid-bed process for recovering uranium from enriched uranium-Zircaloy alloy fuels are in progress. The initial step involves hydrochlorination of the fuel while it is submerged in an inert fluidized bed of solids. The zirconium, converted to the volatile tetrachloride, passes as a waste stream to other waste processing equipment. This results in separation of uranium from the zirconium, since the uranium is retained in the fluid bed as the solid trichloride. Fixed beds of granular material (currently Norton Alundum) are being tested as high temperature filters for removal of the solid uranium trichloride. The uranium is fluorinated to the hexafluoride, volatilized out of the system and recovered.

Evaluation of a combined up-flow and down-flow filter bed system in series with the reaction (fluidized) bed is in progress. Initial results showed 0.1 percent uranium loss of the uranium charge, similar to that achieved in separate up-flow and down-flow filter tests reported in the November, 1961 Progress Report. The first complete uranium material balance made on a hydrochlorination of uranium-zirconium alloy indicated that essentially all of the uranium which reacted remained in the reactor system, thus confirming the low loss data. The major portion of uranium remained in the beds while approximately ten percent of it was on reactor surfaces. Several stainless steel components of the system suffered severe corrosion during hydrochlorination-fluorination cycles; they are being replaced with nickel components.

(2) Fluid-Bed Hydrolysis of Zirconium Tetrachloride - In a proposed process for recovering uranium from low uranium-Zircaloy alloys, the primary off-gas will contain volatile zirconium tetrachloride produced during hydrochlorination of the alloy. The conversion of zirconium tetrachloride to zirconium dioxide by reaction with steam in a fluid-bed reactor is being studied as a means of processing this off-gas. Current studies are investigating whether the reaction occurs principally on the surface provided by the bed particles or in the gas phase. Initial tests with beds of sand indicated the reaction occurred primarily in the gas phase. Other bed materials will be tested.

## 2. General Chemistry and Chemical Engineering

a. Conversion of Uranium Hexafluoride to Uranium Dioxide - Two-Step Fluid-Bed Process - In attempts to minimize solids deposition on reactor surfaces during the reaction of steam with uranium hexafluoride, operations at higher temperatures (500°C rather than 200°C) are being

tested. Preliminary results after  $3\frac{1}{2}$  hours of running with a hexafluoride rate of 100 g/min and a 90-10 steam-hydrogen stream gave a black product indicative of  $U_3O_8$ .

Analyses of powder samples taken without exposure to air from one of the long uranyl fluoride production runs showed water contents (by Karl Fisher method) of 0.016 percent in the bed material and 0.18 percent in the overhead fines. X-ray diffraction analyses of the fines gave patterns of only anhydrous uranyl fluoride.

b. Preparation of Uranium Monocarbide - A total of 1500 grams of uranium monocarbide was prepared in three batches by addition of carbon to zinc-magnesium solutions of uranium. Dry grinding and vacuum sintering resulted in a product with a density of 88 percent of theoretical. Metallographic examination indicated traces of uranium metal, but no uranium dicarbide. Preliminary efforts to produce uranium monocarbide by precipitation from liquid cadmium have not proved successful.

### 3. Chemical-Metallurgical Process Studies

a. Liquid Metal Solvent Studies - The solubility of uranium in liquid indium over the range of  $455^\circ$  to  $720^\circ\text{C}$  may be represented by the equation

$$\log (\text{atom percent uranium}) = 3.78 - 5150 T^{-1}$$

The solid phase in equilibrium with the solution was found to be  $UIn_3$ .

The coprecipitation of ruthenium by uranium from magnesium-zinc solutions has been discussed previously (see October Progress Report, ANL-6454). It was noted that the results indicated that the coprecipitation coefficient of ruthenium by  $\gamma$ -uranium was different from the coefficient for  $\beta$ -uranium. The present study was undertaken to verify these findings. Provisional values for the coprecipitation coefficient of ruthenium by uranium from magnesium-zinc solution are 0.3 at  $752^\circ\text{C}$  and 0.8 at  $810^\circ\text{C}$ . At  $752^\circ\text{C}$ ,  $\beta$ -uranium is believed to be the carrier, whereas at  $810^\circ\text{C}$ ,  $\gamma$ -uranium is probably the carrier.

The mutual solubility of lead and zinc from  $650^\circ$  to  $802^\circ\text{C}$  was measured by sampling the coexistent liquid phases. The data indicate that the consolute temperature is above  $784^\circ$  and below  $802^\circ\text{C}$ .

The free energy (Gibbs) of formation of the uranium-tin intermetallic compound  $USn_3$  was determined as a function of temperature over the range of  $373^\circ$  to  $677^\circ\text{C}$  by means of the galvanic cell method. The free energy of formation  $\Delta G_f^\circ$  may be represented by the following equation

$$\Delta G_f^\circ (\text{cal/mole}) = -39,180 + 9.499 T + 3.062 \times 10^{-4} T^2$$



At 500°C,  $\Delta G_f^\circ = -31.65$  kcal/mole, the enthalpy  $\Delta H_f^\circ = -39.0_0$  and the entropy of formation  $\Delta S_f^\circ = -9.97$  cal/(deg K)(mole).

The phase relations in the lanthanum-cadmium system were studied by means of the recording effusion balance. The study confirmed the existence of  $\text{LaCd}_{11}$  and  $\text{LaCd}_2$ . A new phase,  $\text{La}_2\text{Cd}_9$ , was found. All three phases appeared to have quite narrow ranges of homogeneity. No evidence of the existence of  $\text{LaCd}_6$  and  $\text{LaCd}_3$  was found, although their existence might be expected from the behavior of other light rare earth-cadmium systems.

b. Calorimetry - A value of  $-270.10 \pm 0.24$  kcal/mole was obtained for the standard heat of formation  $\Delta H_f^\circ(25^\circ\text{C})$  for boron trifluoride gas.

Calorimetric studies to determine the heat of formation of hexagonal boron nitride have been completed. A revised value of  $-210.46 \pm 0.68$  kcal/mole was obtained for the heat of combustion of hexagonal boron nitride with fluorine. When this value is combined with the value for the heat of formation of boron trifluoride gas ( $-270.10 \pm 0.24$  kcal/mole), a value of  $-59.64 \pm 0.72$  kcal/mole is obtained for the heat of formation  $\Delta H_f^\circ(25^\circ\text{C})$  for hexagonal boron nitride.

Calorimetric studies to determine the heat of combustion of silicon powder and of large crystals of silicon have been completed. After corrections for impurities were made, eight experiments with powdered silicon (less than 100 mesh) gave a value for the heat of combustion of  $-13.708 \pm 0.009$  kcal/g and five runs with the large crystals of silicon gave a heat of combustion of  $-13.721 \pm 0.008$  kcal/g. The value obtained for the large crystals of silicon is considered to be more reliable since the amount of impurities in the large crystals was much smaller (about  $\frac{1}{6}$ ) than in the powdered silicon. A preliminary value for the standard heat of formation of silicon tetrafluoride was found to be  $-386.02 \pm 0.24$  kcal/mole for the reaction  $\text{Si}(c) + 2\text{F}_2(g) = \text{SiF}_4(g)$ . This value differs considerably from the value ( $-372.9$  kcal/mole) reported elsewhere.<sup>1</sup>

Preliminary values for the heats of formation of both amorphous (glassy) silica and alpha-quartz were obtained. The heat of formation  $\Delta H_f^\circ(25^\circ\text{C})$  for glassy silica was found to be  $-215.98 \pm 0.30$  kcal/mole and a value of  $-217.76 \pm 0.34$  kcal/mole was obtained for alpha quartz. The new value for alpha-quartz differs considerably from the older accepted value of  $-209.9$  kcal/mole, and substantiates the belief that the older value is in error.

---

<sup>1</sup> Joint Army-Navy-Air Force Interim Thermochemical Tables, Vol. 2, December 31, 1960, compiled by the Dow Chemical Company, Thermal Laboratory, Midland, Michigan.



Values for the heats of combustion and heats of formation of zirconium hydride and zirconium deuteride (see October Progress Report, ANL-6454) were revised after corrections were made for the impurities (mainly oxygen) in the samples. The revised values are as follows: (1) the standard heat of combustion  $\Delta E_c^\circ(25^\circ\text{C})$  for zirconium hydride is  $-3123 \pm 3.26$  cal/g and the heat of formation  $\Delta H_f^\circ(25^\circ\text{C})$  is  $-37.72 \pm 0.72$  kcal/mole; and (2) the standard heat of combustion for zirconium deuteride is  $-3066.22 \pm 2.63$  cal/g and the heat of formation is  $-39.00 \pm 0.64$  kcal/mole.

From a preliminary series of combustions of magnesium in fluorine, a tentative value of  $-265$  kcal/mole was obtained for the heat of formation of magnesium fluoride. An additional series of runs is being planned in which refinements in technique are expected to yield results of higher accuracy.

## F. Advanced Reactor Concepts

### 1. Fast Reactor Test Facility (FARET)

The general engineering and physics parameters for an experimental facility to test characteristics of advanced fast reactors are being examined. These studies are directed toward a preliminary design of a test facility showing general feasibility.

a. Facility Design - The reactor vessel has been redesigned to guide the incoming sodium down an annulus for maintaining lower reactor vessel wall temperature. Thus high operating coolant temperatures may be achieved while permitting the use of conventional materials (AISI Type 316 stainless steel) for the reactor vessel.

To maintain the sodium purity at all times a cold trap and a hot trap system has been proposed. Approximately 50 gpm (3 liter/sec) of sodium will be bypassed to the cleanup system. The cold trap would be employed for system temperatures less than  $1200^\circ\text{F}$  ( $650^\circ\text{C}$ ) and the zirconium hot traps for higher temperatures.

b. Heat Transfer, Fluid Flow, Stress Analysis - A more detailed analysis was made of the sodium leakage problem at the discharge plenum region of the reactor vessel (discussed in ANL-6473, Progress Report for November, 1961). The leakage is due to the clearance between the hexagonal fuel element extensions and to the plenum pressure which forces the sodium through the primary heat exchanger. The advantage of the pressure breakdown principle at this point lies in its independence of sodium level control in the reactor vessel, which would be necessary for gravity flow. It was found that the leakage flow rates would be approximately

8% of the total maximum primary system flow rate for clearances between the fuel element extensions of the order of  $\frac{1}{32}$  in. (0.08 cm), a plenum pressure of 3 psig (0.21 kg/cm<sup>2</sup>), and a core of 300 EBR-II size assemblies. In addition, approximately 6% of the reactor inlet flow rate (at temperature = 650°C) would have to be mixed with the leakage flowrate (temperature = 760°C) to maintain the reactor vessel wall temperature and corresponding allowable code stress to acceptable values for limiting modes of operation [700°C, 3500 psi (250 kg/cm<sup>2</sup>)]. The bypass flow rate (14% of total) would be returned to the main coolant pump tank. Further studies are in progress to effect a reduction in the bypass flow rate.

c. Shielding Analysis - A study was made to determine the effect of a two-foot magnetite shield enclosing the control rod mechanism space immediately above the top cover of the reactor vessel. The rod mechanisms in the enclosure were assumed to be irradiated by a neutron flux which penetrates a 6-in. (15-cm) thick steel top cover plate. The maximum fast flux leaving the magnetite shield was calculated to be  $5 \times 10^5$  n/(cm<sup>2</sup>)(sec). Schemes are being studied to reduce this flux by a combination of additional shielding and distance.

The flux above the steel top cover was determined to be  $7.2 \times 10^6$  n/(cm<sup>2</sup>)(sec). It was estimated that the radiation from the activity of the steel of the cover and that of the control mechanisms could still be tolerated after one year of operation.

d. Reactivity Coefficients - Reactivity effects of an oxide fueled, sodium-bonded and cooled core due to change in fuel density with temperature have been completed for various compositions and sizes. The results are listed in Table XIII for various fuel/coolant/structure composition, enrichment, volume, and L/D ratios. The reactivity change is based on calculated systems whose temperatures differ by about 2000°C. The effect of displacement of sodium due to the radial expansion is included in the computation. This increases the magnitude of the negative coefficient by something less than 5%. The reactivity change appears to be a linear function of the initial radial leakage.

Table XIII. Fuel Expansion Coefficient for FARET-Type Oxide Cores

Core Volume Fraction Composition PuO <sub>2</sub> -UO <sub>2</sub> /Na/Nb	Enrichment in % Pu	Volume in Liters	L/D	Core Leakage		$\Delta K/kT/T$
				Radial	Axial	
40/50/10	23.2	234	1.26	.354	.107	$-1.397 \times 10^{-5}$
50/37.5/12.5	17.9	263	1.19	.302	.096	$-1.227 \times 10^{-5}$
66/18/16	13.6	310	1.09	.2346	.082	$-9.512 \times 10^{-6}$
50/37.5/12.5	13.6	673	1.123	.220	.073	$-8.804 \times 10^{-6}$
66/18/16	13.6	304	.88	.212	.103	$-8.70 \times 10^{-6}$
40/50/10	13.6	1300	1.10	.212	.075	$-8.12 \times 10^{-6}$
40/50/10	13.6	1520	.472	.119	.139	$-5.3 \times 10^{-6}$

## 2 Direct Conversion Studies

The cell described in the Progress Report for March, 1961 (ANL-6343) was used with a tantalum emitter and potassium vapor. The collector consisted of silver oxide on copper. The voltage-current characteristics of the cell were taken with an X-Y recorder, and the voltage-power characteristics were plotted showing the power maximum. The temperatures were varied during each series, while the potassium pressure was kept approximately constant. Next the potassium pressure was changed and the temperature variations repeated.

Three typical graphs are shown for different temperatures and pressures in Figures 6, 7 and 8. The graphs look very similar to those obtained with cesium plasma cell. Power is delivered by the cell if the collector is negative relative to the emitter, i.e., at negative voltages. The voltage close to the sharp dip of the current gives approximately the difference of the emitter-collector work function  $\phi_E - \phi_C$ , as was discussed.  $\phi_E - \phi_C$  is about 2.4 to 2.6 volts and if no losses in the plasma occur, this is practically the voltage for the power maximum. The work function of pure tantalum is usually given as 4.1-4.2 volts. However electron emission of the tantalum emitter actually used gave a somewhat higher value of 4.4 volts.

Since the collector was cooled with silicon oil, the thin layer of potassium probably covered the collector and reduced the collector work function considerably. These effects were observed with the cesium cells. Negative sections of the voltage-current characteristics were observed frequently for different temperatures and pressures. The experiments are still in progress.

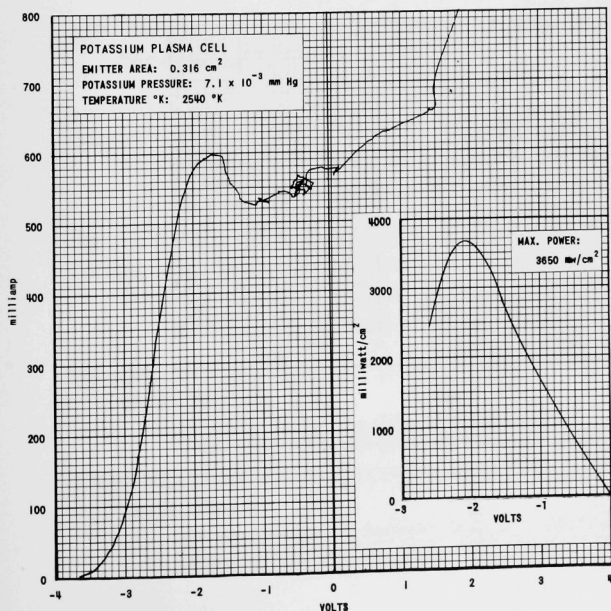


Figure 6  
Current and Power  
Characteristics of  
Potassium Cell

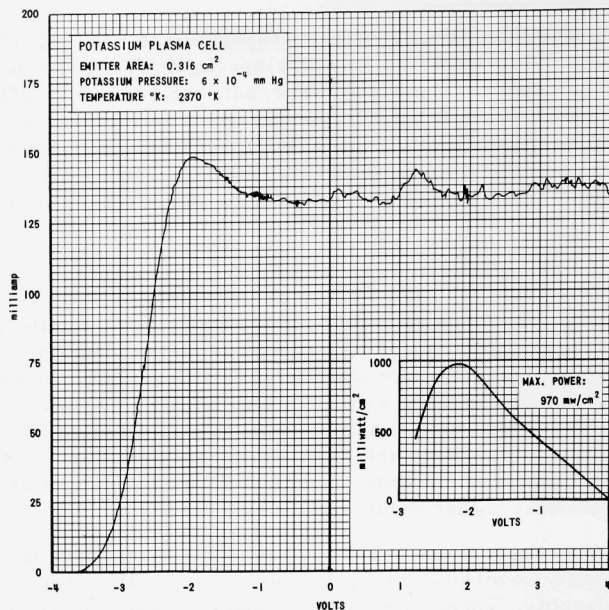


Figure 7. Current and Power Characteristics of Potassium Cell

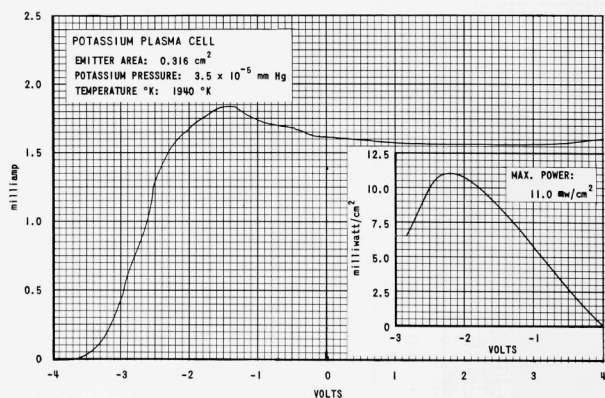


Figure 8. Current and Power Characteristics of Potassium Cell

## V. PUBLICATIONS

### Papers

#### VOID MEASUREMENT IN A BOILING REACTOR

J. A. Thie, J. Beidelman, and B. Hoglund

Nuclear Science and Engineering, 11, No. 1-6 (1961).

#### TWO-PHASE FRICTIONAL PRESSURE DROP PREDICTION FROM LEVY'S MOMENTUM MODEL

J. F. Marchaterre

Heat Transfer 83 (4) 503-505 (Nov 1961).

#### FAST-NEUTRON-INDUCED FISSION CROSS SECTIONS OF Pu-241 AND Am-243

Daniel K. Butler and Ruth K. Sjoblom

Physics Review 124, pp. 1129-1131 (1961).

#### LOW-TEMPERATURE PHASE TRANSITION IN ALPHA URANIUM

E. S. Fisher and H. J. McSkimin

Phys. Rev. 124 (1) 67-70 (1961).

#### ADIABATIC ELASTIC MODULI OF SINGLE CRYSTAL ALPHA ZIRCONIUM

E. S. Fisher and C. J. Renken

J. Nuc. Matls. 4 (3) 311-315 (1961).

#### ZIRCONIUM ALLOYS FOR USE IN SUPERHEATED STEAM

Sherman Greenberg

J. Nuc. Matls. 4 (3) 334-335 (1961).

#### GLASSY MATERIALS FOR NUCLEAR REACTOR APPLICATIONS

J. H. Handwerk, E. D. Lynch and V. K. Moorthy

Indus'l. Heating 28, 2258 (1961).

#### OXIDATION AND PHASE STABILITY IN THE SYSTEM URANIUM OXIDE-LANTHANUM OXIDE

David C. Hill

Indus'l. Heating 28, 2260 (1961).

#### US AND ThS BODIES

P. D. Shalek

Indus'l. Heating 28, 2260 (1961).

#### FABRICATION OF PLUTONIUM FAST REACTOR FUELS

A. B. Shuck

Proceedings of Annual Nuclear Materials Management Meeting,  
Denver, Colorado, June 15, 1961. TID-7615, 102-120 (1961).

PROGRESS IN NUCLEAR ENERGY, SERIES IX, ANALYTICAL CHEMISTRY, VOL 2

C. E. Crouthamel, Ed.

London: Pergamon Press, 1961.

RECENT ADVANCES IN COUNTING TECHNIQUES (CHAPTER I)

C. Gatrousis, R. Heinrich, and C. E. Crouthamel

Progress in Nuclear Energy, Series IX, Analytical Chemistry, Vol. 2, C. E. Crouthamel, Ed. London: Pergamon Press, 1961.

VERSATILE SCRUB TOWER REMOVES HALOGEN OFF-GAS

J. Holmes

Chem. Eng. 68 (No. 26), 94 (1961).

SOME RECENT DEVELOPMENTS IN FLUID-BED CALCINATION EQUIPMENT

A. A. Jonke

Fixation of Radioactivity in Stable, Solid Media, Report of Second Working Meeting at Idaho Falls, September 27-29, 1960, TID-7613, (February 1961).

PRELIMINARY STUDIES ON FLUID-BED CALCINATION OF PUREX PROCESS WASTE

A. A. Jonke, J. W. Loeding and L. J. Anastasia

Fixation of Radioactivity in Stable, Solid Media, Report of Second Working Meeting at Idaho Falls, September 27-29, 1960, TID-7613, (February 1961).

THE KINETICS OF OXIDATION OF URANIUM BETWEEN 125 AND 250°C

L. Liebowitz, J. G. Schnizlein, J. D. Bingle and R. C. Vogel

J. Electrochem. Soc. 108, 1155 (1961).

A MICROSCOPIC STUDY OF OXIDE FILMS ON URANIUM

L. Liebowitz, J. G. Schnizlein, L. Mishler and R. C. Vogel

J. Electrochem. Soc. 108, 1153 (1961).

THE EFFECT OF AN ELECTRICAL DISCHARGE ON OXIDATION KINETICS OF URANIUM

J. G. Schnizlein, J. D. Bingle and L. Liebowitz

J. Electrochem. Soc. 108, 1166 (1961)

ANL Reports

ANL-6248-  
Addendum

TERMINAL REPORT ON THE BOILING SLURRAY  
REACTOR EXPERIMENT (SLURREX) Mockup  
Hydraulic Experiments  
Joseph D. Lokay

- ANL-6342      A PROCESS FOR THE RECOVERY OF URANIUM  
FROM NUCLEAR FUEL ELEMENTS USING FLUID-  
BED DRYING AND VOLATILITY TECHNIQUES  
N. Levitz, J. Barghusen, E. Carls and A. A. Jonke
- ANL-6344      EFFECTS OF ROLLING AND HEAT TREATMENT ON  
ANISOTROPIC IRRADIATION GROWTH OF URANIUM  
J. H. Kittel
- ANL-6403      FAST REACTOR SHAPE FACTORS AND SHAPE-  
DEPENDENT VARIABLES  
W. B. Loewenstein and G. W. Main
- ANL-6436      AN ANALYSIS OF SPECIFIC HEAT DATA FOR WATER  
AND WATER VAPOR IN THE CRITICAL REGION  
E. S. Nowak and R. J. Grosh
- ANL-6437      AN EVALUATION OF REACTOR CONCEPTS FOR USE  
AS SEPARATE STEAM SUPERHEATERS  
D. H. Lennox, D. R. MacFarlane, R. C. Brubaker,  
E. L. Martinec, R. R. Rohde, B. J. Toppel, and  
H. Unger
- ANL-6442      COST FUNCTION STUDIES FOR POWER REACTORS  
J. Heestand and L. T. Wos
- ANL-6443      A SUMMARY OF SHIELDING CONSTANTS FOR  
CONCRETE  
R. L. Walker and M. Grotenhuis
- ANL-6466      EFFECT OF RESONANCE SCATTERING ON CRITI-  
CALITY CALCULATIONS OF FAST ASSEMBLIES  
D. Meneghetti
- ANL-6468      AN EXPERIMENTAL INVESTIGATION OF SOME  
SOURCES OF ERROR IN THE MEASUREMENT OF  
ABSOLUTE FISSION RATIOS IN FAST REACTORS  
W. G. Davey and R. N. Curran
- A STUDY OF CHEMICAL POISONS FOR NUCLEAR  
REACTOR CONTROL  
Robert Batch  
Technical Memo #25 (Reactor Engineering  
Division), June, 1961.







ARGONNE NATIONAL LAB WEST



3 4444 00007583 8

+